UNIVERSITE DE LIEGE

FACULTE DES SCIENCES APPLIQUEES

RECENT ADVANCES IN THE FIELD OF STEEL JOINTS

COLUMN BASES AND FURTHER CONFIGURATIONS FOR BEAM-TO-COLUMN JOINTS AND BEAM SPLICES

par

J.P. JASPART
Chercheur qualifié du F.N.R.S.

APPENDICES

Thèse présentée en vue de l'obtention du grade d'Agrégé de l'Enseignement Supérieur

Année académique 1996-1997

TABLE OF CONTENTS

APPENDIX 3

DESIGN STIFFNESS AND RESISTANCE PROPERTIES OF BOLTED JOINTS MAY BE SIGNIFICANTLY INCREASED BY THE ADDITIONAL CONSIDERATION OF THE BOLT HEAD SIZE AND THE BOLT PRELOADING

APPENDIX 1

THERE IS A SIGNIFICANT RISK OF INCONSISTENCY WHEN COMPARING TEST RESULTS WITH PREDICTION MODELS FOR JOINTS

1. INTRODUCTION

The resistance of any structural element appears traditionally as the most important mechanical property to consider in the design process. Its precise evaluation through appropriate tools (analytical formulae, laboratory tests, finite element simulations, ...) is a prerequisite to an economical and safe structural design.

This statement is agreed by all, but the definition to give to the term « resistance » seems to differ substantially from one person, one institution or one country to another. This situation is quite embarrassing for different reasons :

- The tools proposed in the literature for the evaluation of the resistance have to be first validated through comparisons with test results and the compared values should obviously refer to the same definitions.
- When the evaluation tools for resistance are codified or recommended in design handbooks, their use should be made in a appropriate way.
- The level of resistance to be considered in the design process depends on the type of frame analysis which is performed, and any inconsistency should be avoided.

The terms used to define the resistance are quite important. Expressions like : "design resistance", "actual resistance", "ultimate resistance", "plastic resistance", ... seem not to be understood in a similar way over the world.

In this particular context, it appears quite necessary, through the present annex, to clarify the different terms listed here above and to define them in a proper way so to avoid confusions and misunderstandings.

All the definitions are illustrated in the particular case of structural joints; they however apply to any structural element and can therefore be easily generalized.

2. DEFINITIONS

A clear distinction has to be made first between resistances obtained through laboratory tests and through the application of analytical or numerical models.

2.1 Resistances from tests

In laboratory tests, moment-rotation curves are traditionally reported. Their shape differs from one specimen tested to another, but three main rotational responses may be identified :

- M-ϕ curves with quite infinite ductility (Figure 1.a);
- M-ϕ curves with good but finite ductility (Figure 1.b);

- M-ϕ curves with quite limited ductility (Figure 1.c).

The maximum resistance than the joint is able to transfer is said ***ultimate*** and named $M_{Ru,test}$.

For the first category (Figure 1.a), the ductile behaviour is such that the ultimate moment resistance of the joint can not be reached during the test, often because of too high displacements in one of the connected members. The ultimate resistance can therefore not to be reported and remains unknown.

For the second and third categories (Figure 1.b and 1.c), the ultimate resistance is reached because of the brittle failure - bolts for instance - or the local instability - column web in compression, beam flange and web in compression - of one of the constitutive components of the joint. The value of the ultimate resistance is so clearly identified.

The ductile response of the joint is the result of the progressive yielding of one or more of the components. The stresses extend far beyond the yield stress of the materiel, so developing strain-hardening. This provides to the moment-rotation curves a bi-linear response as shown in Figure 1.a. In some cases, this progressive yielding is interrupted by the brittle failure or the instability of a component, what limits the ductility and the bi-linear character of the curves, as illustrated in Figure 1.b and 1.c.

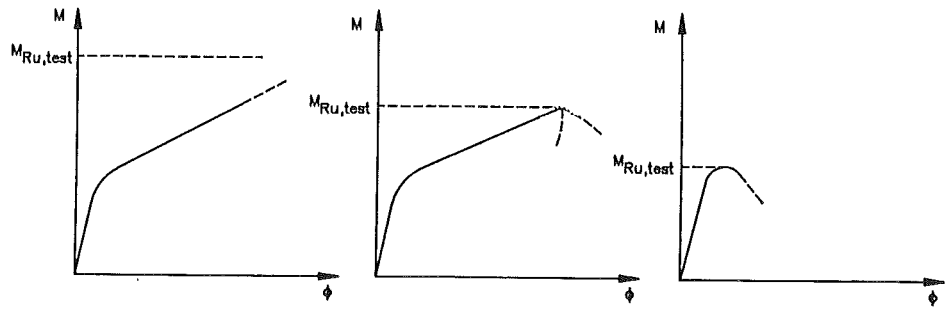

(a) Quite infinite ductility (b) Good but finite ductility (c) Quite limited ductility

Figure 1 Ultimate resistance from tests

Figure 2 points out the influence of the strain hardening on the moment-rotation curves. For a perfectly elastic material, the moment-rotation would peak at a resistance level named $M_{Rp,test}$, which can be roughly defined as the plastic resistance of the joint. The word "plastic" is quite appropriate as long as yielding phenomena develop and the full plastic resistance of the joints is reached, as for beam and column sections. This is the

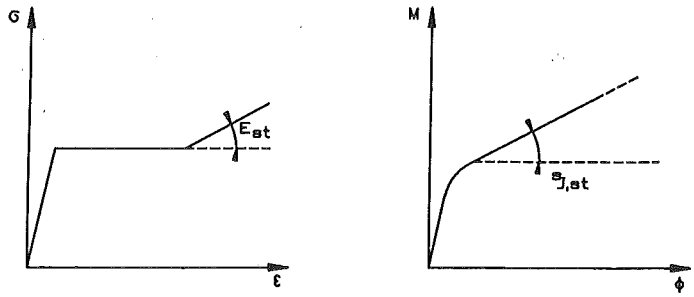

σ-ε curve M-ϕ curve

Figure 2-2 Influence of strain-hardening

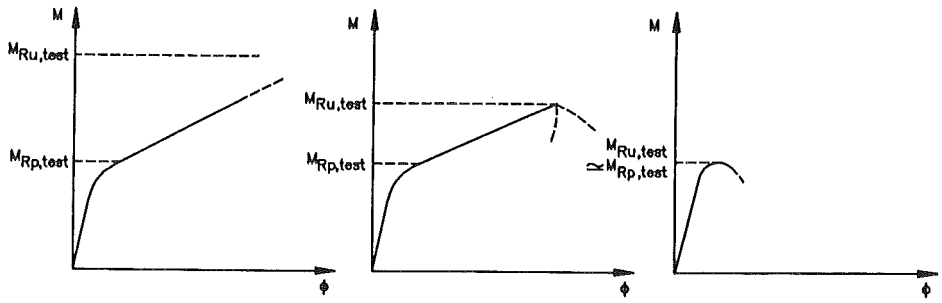

(a) Quite infinite ductility (b) Good but finite ductility (c) Quite limited ductility

Figure 2-3 Ultimate and pseudo-plastic resistances from tests

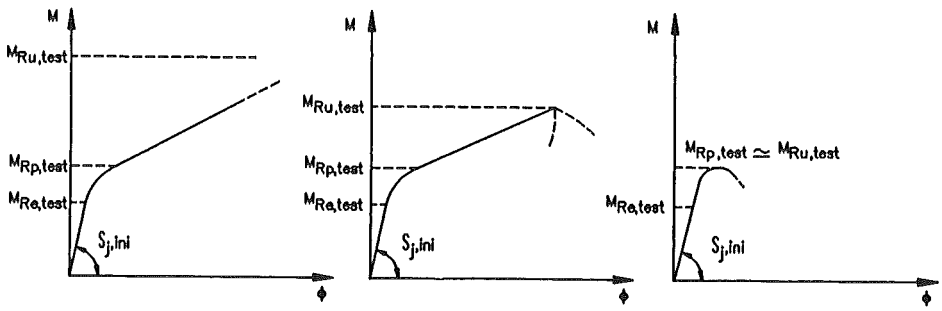

(a) Quite infinite ductility (b) Good but finite ductility (c) Quite limited ductility

Figure 2-4 Ultimate, pseudo-plastic and elastic resistances from tests

case for category 1 and 2 curves (see Figure 3.a and 3.b). In category 3 curves, no strain-hardening occurs and the two $M_{Rp,test}$ and $M_{Ru,test}$ values coincide; the word "plastic" is still justified if the buckling or the instability occurs just after the plastic resistance of the joint is reached. It is no more acceptable for joints where the instability phenomena or brittle failures precedes the full plasticity. This is why it is suggested here to define $M_{Rp,test}$ as the "**pseudo-plastic**" resistance of the joint but keep anyway the subscript p for simplicity.

Lastly, the maximum **elastic** moment resistance $M_{Re,test}$ of the joint may be usually identified, together with the initial elastic rotational stiffness $S_{j,i}$. (Figure 4).

For sake of completion, it has to be mentioned that membranar effects may sometimes develop in constitutive joint components, as a result of their yielding and of the corresponding deformation (as in thin end-plates and flange cleats in bending, for instance). The strain hardening stiffness $S_{j,st}$ is so increased by a this membranar contribution $S_{j,m}$ as pointed out in Figure 5. The stiffness characterizing the second branch of the M-ϕ curve located beyond $M_{Rp,test}$ is therefore said "post-limit" ($S_{j,post-limit}$ in Figure 5).

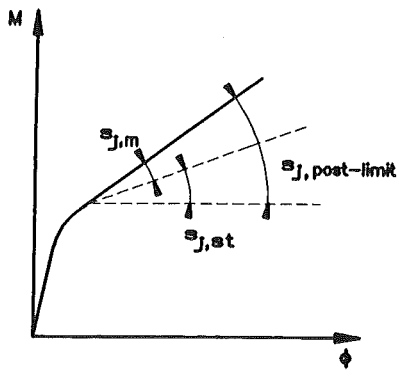

Figure 5 Definition of the post-limit stiffness

2.2 Resistances from models

In order to validate prediction tools for resistance, comparisons with tests are usually performed. For sake of consistency, quantities corresponding to similar definition have to be compared. The appropriate moment resistances from the tests and from the models have therefore to be selected, according the level of sophistication of the model.

The more sophisticated models provide the user with a full non-linear curve covering the successive loading steps from the first beginning to failure. Before using these models, the **actual** values of the mechanical steel properties for all the joints components are measured; they are used further as data for the models. The **pseudo-plastic** resistances

from tests and models can then be directly compared. Similar test-model comparisons can be carried out with **ultimate** resistances, as long as the $M_{Ru,test}$ value can be derived. This requires the measurement of the actual ultimate stress values in order to derive the ultimate yielding resistance. Local instabilities can obviously limit the ultimate joint resistance to a lower value, as for category 2 and 3 curves. The evolution of the rotational stiffness is also often predicted by the sophisticated models. A direct comparison between full non linear curves from test and model can therefore be contemplated (see Figure 6).

Less sophisticated models exist; they allow to derive the **pseudo-plastic** and/or the **ultimate** resistances only. For design purposes, strain-hardening and membranar contributions to the moment resistance are systematically neglected, so limiting the transfer of moment between the connected members to $M_{Rp,model} \approx M_{Rp,test}$. The concept of plastic hinge idealization is so followed, and the length of the yield plateau, which decreases from categories 1 to 3, as shown in Figure 7, determines the so-called available plastic rotation of the joint.

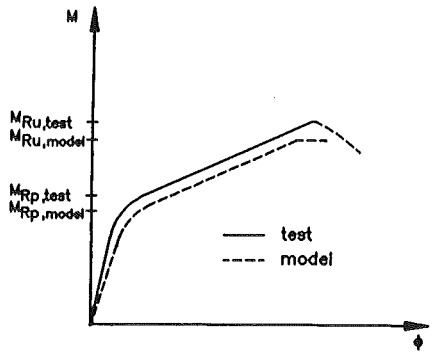

Figure 6 Possible comparisons between models and tests

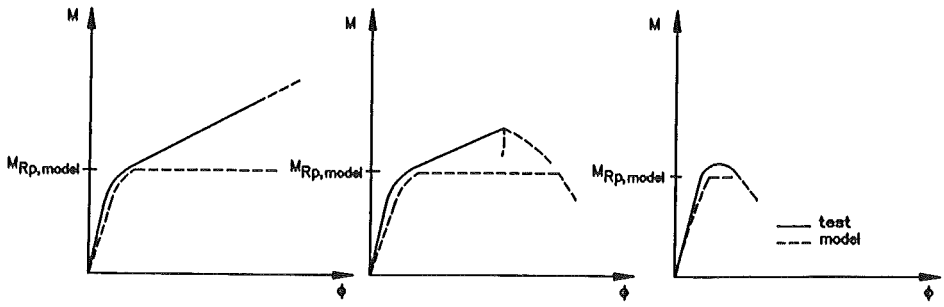

Figure 7 Plastic hinge idealization

In a usual design process, the actual values of the yield stresses are unknown and reference has to be made to characteristic values sometimes called "nominal". The introduction of these characteristic values into prediction models allow to derive **characteristic** moment resistances M_{Rk}.

Furthermore, modern codes, as Eurocodes, follow a semi-probabilistic approach for structural safety. The resistance to be used accordingly are design ones and not characteristic ones. They are obtained through the application of the above mentioned models in which design values of the yield stresses are introduced. These ones are derived quite easily by dividing the **characteristic** values of the yield stresses by an appropriate partial safety factor γ. The so-defined **design** moment resistance is named M_{Rd}.

In the case of components exhibiting a quite brittle behaviour (bolts in tension, welds, ...), it has to be mentioned that it is referred to f_u and not f_y in the expressions of their pseudo-plastic, characteristic and design resistances, what is not surprising for such "category 3" components.

3. CONCLUSIONS

Figure 8 illustrates the test and model moment resistances which are defined in the present annex in the particular case of the Eurocode tri-linear model for joints. It indicates that the only comparisons which can be carried out between tests in laboratory and the Eurocode model are on "**pseudo-plastic**" values ($M_{Rp,test}$ and $M_{Rp,model}$).

To derive $M_{Rp,model}$, actual measured values of the yield (or ultimate for brittle components) stresses and partial safety factors γ_{M0} (steel), γ_{Mb} (bolts), γ_{Mc} (concrete) and γ_{Mw} (welds) equal to 1,0 have to be considered.

From the models giving $M_{Rp,model}$, characteristic and design moment resistances can then be derived. The latter are those of interest for practical design purposes.

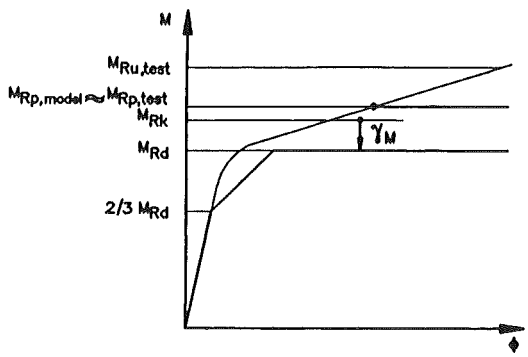

Figure 8 Test and model moment resistances

APPENDIX 2

THE "PLASTIC HINGE IDEALIZATION" FOR STRUCTURAL JOINTS IS SUBORDINATED TO A SET OF SPECIFIC JOINT REQUIREMENTS

1. INTRODUCTION

1.1 Generals

Structural joints exhibit a non-linear behaviour when subjected to high bending moments. This non-linear response of the joints is expressed in the form of a characteristic M-ϕ curve (Figure 1) where M represents the applied moment and ϕ the relative rotation between the two connected members.

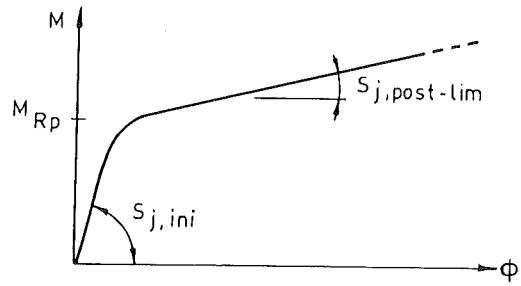

(a) Infinitely ductile behaviour

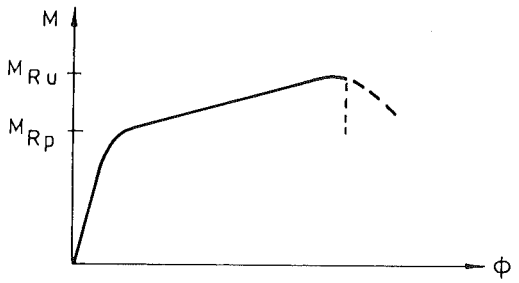

(b) Limited ductility

(c) Non-ductile behaviour

Figure 1 Shape of actual joint M-ϕ curves

For most of the structural joints, the shape of these characteristic M-ϕ curves is rather bi-linear (Figure 1.a). The initial slope corresponds to the elastic deformation of the joint ($S_{j,ini}$). It is followed by a progressive yielding of the joints (of one or some of the constitutive components) until the so-called pseudo-plastic resistance M_{Rp} (defined in Appendix 1) is reached. Then develops a post-limit behaviour ($S_{j,post\text{-}lim}$) which corresponds to the development of strain-hardening and possibly membrane effects. The latter are of particular high importance in components where rather thin plates are subjected to transverse tensile forces as, for instance, in minor axis joints and joints with columns made of rectangular hollow-sections.

In a lot of experimental tests (Figure 1.a), the failure of the joints (M_{Ru}) is not reached because of high local deformations in the joints resulting in extremely high relative rotations. In the other tests (Figure 1.b), the failure is reached by excessive yielding or, more often, by instability of one of the constitutive components (for instance, the buckling of the column web panel in compression or of the beam flange and web in compression) or by brittle failure in the welds or in the bolts. For some joints, the premature failure of one of the components prevents the development of a high moment resistance and high rotation. The post-limit range is rather limited and the bi-linear character of the M-ϕ curve is less obvious to detect (Figure 1.c).

1.2 Joint idealization

In view of the frame design and analysis, two attitudes may be followed :

- the non-linear M-ϕ curves are dealt with in the calculations, what requires the use of non-linear analysis softwares to derive the internal forces in the structural elements and joints;

- the non-linear M-ϕ curves are idealized (Figure 2) so as to allow, for instance, a more simple elastic or rigid-plastic analysis to be performed.

In the revised Annex J of Eurocode 3 [1], guidelines are given on how to perform these idealizations. In particular, the concept of plastic hinge commonly used for beam and column sections has been extended to joints. The three following features characterize the idealized curves as reported in Figure 2:

- a stiffness idealization for moments ranging between 0 and M_{Rd};

- a design resistance M_{Rd} (defined in Appendix 1);

- a yield plateau which justifies the term "plastic hinge idealization"; its length corresponds to the available plastic rotation capacity, if any.

From these definitions, the parallelism with the idealization of the beam or column cross-sections in bending is quite obvious.

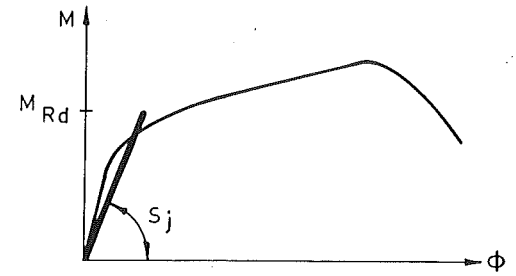

(a) Linear idealization

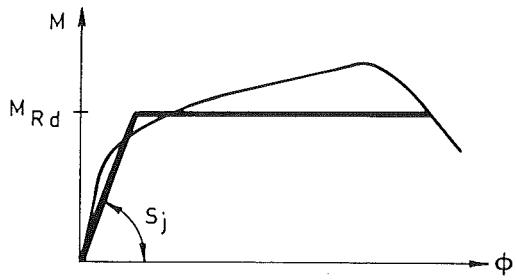

(b) Bi-linear idealization

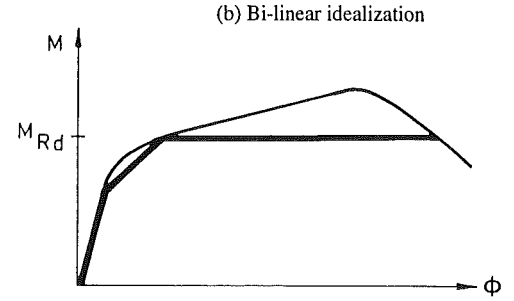

(c) Tri-linear idealization

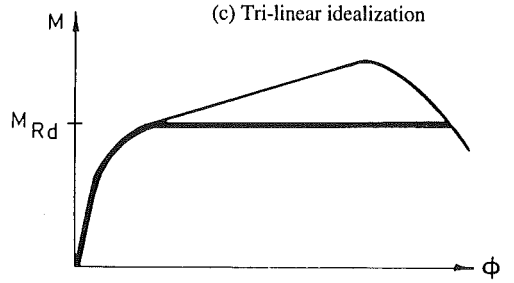

(d) Non-linear idealization

Figure 2 Joint idealizations for design

Such joint idealizations allow, as for beam and columns, to distinguish between:

Class 1 joints: able to reach M_{Rd} and possessing a sufficiently good rotation capacity for a structural plastic design.

Class 2 joints: able to reach M_{Rd} but characterized by a reduced plastic rotation capacity. A plastic verification of the joint is anyway allowed.

Class 3 joints: where brittle failure (or instability) limits the moment resistance and does not allow a full redistribution of the internal forces in the joint.

The idealizations for class 1 joints - as those represented in Figure 2 - are achieved by fully neglecting the extra strength resulting from the post-limit stiffness.

For beam and column sections, this assumption is widely accepted. In comparison with the yield plateau, the development of a post-limit stiffness slightly affects the redistribution of internal forces in the structure, what is likely to modify the frame response in terms of deflections or failure load; but this influence is so limited that the post-limit stiffness is neglected and the concept of perfect plastic hinge is referred to.

For joints, the situation is quite different; the post-limit stiffness, even when it only results from strain-hardening, is usually much higher than that characterizing the beam and column cross-sections, in terms of percentage of the initial elastic stiffness.

1.3 Values of the post-limit stiffness

As a matter of fact, a joint is constituted of several components, the individual design resistance $F_{Rd,i}$ of which are different each from another. And when the joint is loaded, the weakest component will yield first ($F_{Rd} = min\ (F_{Rd,i})$) and will be responsible for the attainment of M_{Rd}. At this design load level, the other joint components are still elastic, partially yielded or close to reach their own plastic resistance, according the value of $F_{rd,i}$ relatively to F_{Rd}. This situation strongly influences the value of the post-limit stiffness of the joints [2, 3], as demonstrated in the next paragraphs.

For instance, let us assume a joint in which one of the components is much weaker than the others. $S_{j,post\text{-}lim}$ of the joint will result, in such a case, from the combination of the post-limit stiffness of the weak component and the initial stiffness of the others; as a matter of fact, these last ones remain in the elastic range of behaviour for applied moments higher that M_{Rd}.

More usually, the successive apparition of yielding in the different components during the joint loading, beyond M_{Rd}, leads to a progressive decrease of the actual post-limit stiffness in comparison with the previous case. In [2], we explain how to overcome the complexity of the problem; the procedure is briefly explained here below.

Each component which possesses a high design moment resistance in comparison with F_{Rd} will contribute in an elastic way to $S_{j,post\text{-}lim}$. In the contrary, a component, the design

resistance of which is closer to F_{Rd}, will experience strain-hardening, possibly with membrane effects, and will affect more significantly $S_{j,post\text{-}lim}$. The simplified evaluation of $S_{j,post\text{-}lim}$ consists therefore in the classification of the components according to their design resistance $F_{Rd,i}$ in order to distinguish those which will contribute to $S_{j,post\text{-}lim}$ by means of their initial stiffness from those which will contribute by means of their post-limit stiffness. For instance, deep study of experimental tests on joints with endplates [2] has allowed to determine the boundary value of the resistance:

$$F_{Rd,up} = 1{,}65\ F_{Rd}$$

which allows to classify the components (elastic contribution to $S_{j,post\text{-}lim}$ *if* $F_{Rd,i} > F_{Rd,up}$; post-limit contribution if $F_{Rd,i} \leq F_{Rd,up}$).

In the following table, typical values of the ratio $S_{j,ini}/S_{j,post\text{-}lim}$ are given for beam-to-column joints with different connection types.

Joint and connection types	$S_{j,ini}/S_{j,post\text{-}lim}$
• Single-sided major axis beam-to-column with joints end-plate connections (I and H profiles) [2]	25 to 50
• Single-sided major axis beam-to-column joints with flange cleated connections (I and H profiles) [2]	15 to 50
• Single-sided minor axis beam-to-column joints with end-plate connections (I and H profiles) [6]	2 to 9
• Single-sided beam-to-column joints with various connection types [7] (I beams and RHS columns)	3 to 9

Table 1 Values of $S_{j,ini}/S_{j,post\text{-}lim}$

1.4 Influence of the post-limit stiffness of the joints on the frame and joint design

Some values of the $S_{j,ini}/S_{j,post\text{-}lim}$ ratio are so low that the question to know whether it is safe or not to neglect the extra strength of the joint associated to its post-limit stiffness has to be raised.

For what regards this problem, two different aspects have to be considered :

i. The redistribution of internal forces in the frame resulting from the spread of yielding in the members and in the joints is different in reality than that obtained by neglecting post-limit stiffness.

   It is important to mention that the distribution of stiffness in the frame is also altered.

   The first question to raise is therefore to know whether the global frame response (deflections, resistance, stability) is strongly affected or not by the assumption made in design (post-limit stiffness equal to zero), and whether the frame design based on this assumption is conservative (and also not over-conservative).

ii. In reality, the joints have to carry moments higher than M_{Rd} when a hinge is forming, because of this actual post-limit stiffness. Locally, in the joints, some brittle components such as welds and bolts could so be overloaded and could fail. Some guidelines in joint design have therefore be provided to avoid unexpected brittle failures in the joints.

2. PROVISIONS OF EUROCODE 3 ANNEX J

The two different aspects have been taken into consideration in the new revised Annex J for joints developing mainly strain-hardening in the post-limit range (beam-to-column joints or beam splices between H or I profiles and with end-plates, flange cleats,...). The extension of Eurocode 3 Annex J to joints developing also high membrane effects (minor axis joints, joints with tubular columns,...) is not obvious and requires specific verifications.

In the next pages, it is shown how the global and local aspects of the problems are covered in Eurocode 3 Annex J. In [4], we present, together with Vandegans (CRIF), a preliminary study of the possible extension of these provisions to joints developing high membrane effects.

2.1 Global aspects

2.1.1 Joint modelling for frame analysis

In a major axis beam-to column steel joint, two main sources of deformability are identified (Figure 3) [2] :

a) The deformation of the connection, defined as equal to θ_b - θ_c, associated to the deformation of the connection elements (end-plate, angles, bolts,...), to that of the column flange and to the load-introduction deformability of the column web;

b) The shear deformation of the column web associated mostly to the common presence of forces F carried over by the beam(s) and acting on the column web at the level of the joint; these forces are statically equivalent to the beam moment M.

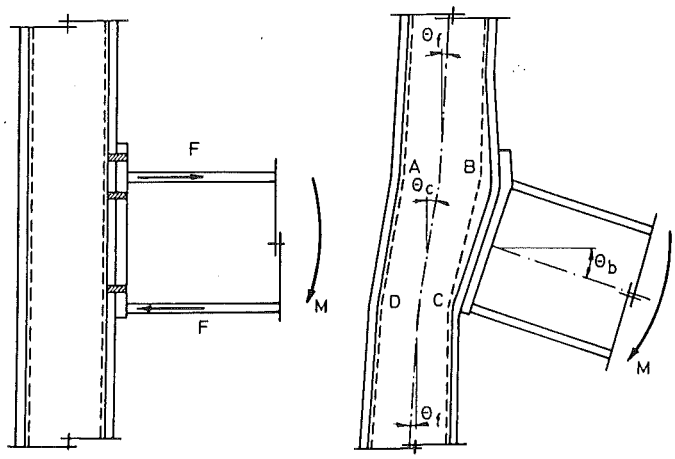

Figure 3 Deformation of a major axis joint

These sources of deformability are illustrated in Figure 4 for the particular case of a joint between a single beam and a column. The deformability of the connection elements is concentrated into a single rotational spring located at the end of the beam (Figure 4.a). The associated behaviour is expressed in the format of an M-ϕ curve.

The deformation of the ABCD column web panel is divided into:

- The load-introduction deformability which consists in the local deformation of the column web in both tensile and compressive zones of the joint (respectively a lengthening and a shortening) and which results in a relative rotation ϕ between the beam and column axes; this rotation concentrates mainly along edge BC (Figure 4.b) and provides also a deformability curve M-ϕ.

- The shear effect - due to shear force V_n - which results in a relative rotation γ between the beam and column axes (Figure 4.c); this rotation makes it possible to establish a second deformability curve V_n-γ.

It is important to stress that the deformability of the connection (connection elements + load-introduction) is only due to the moment(s) carried over by the beam(s) while the shear V_n in a column web panel is the result of the combined action of the equal but opposite forces statically equivalent to be the moment in the beam(s) and of the shear forces in the column.

The difference between the loading of the connection and that of the column web in a specified joint requires, from a theoretical point of view, that account be taken separately of

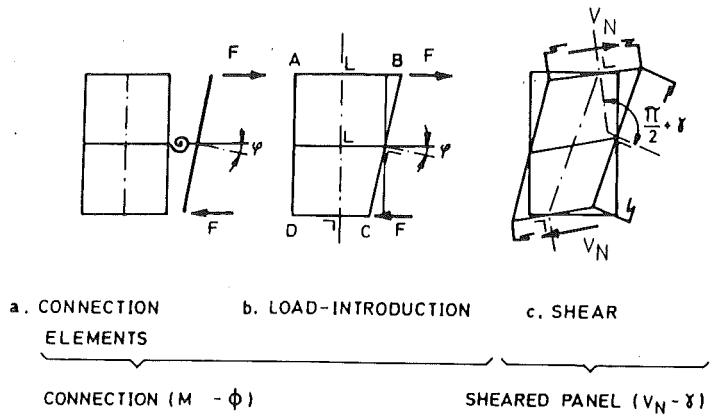

Figure 4 Joint deformability sources

both deformability sources when designing a building frame (Figure 5.a). However doing so is only practicable when the frame is analysed by means of a sophisticated computer program allowing for the separate modelling of both deformability sources. In all the other cases, the actual behaviour of the joints must be simplified by concentrating the whole deformability into a single rotational spring located at the beam-to-column intersection (Figure 5.b), as recommended in Eurocode 3.

Furthermore, the use of non-linear curves for the characterization of the joint behaviour is quite incompatible with a practical design of steel frames. This means that the moment-rotation curve associated to the single flexural spring has to be idealized.

This topic is largely discussed in Chapter 4 of the present thesis.

Based on an extended parametric study of braced and unbraced frames that we have performed in [2] by means of the non-linear finite element program FINELG, the safe and rather accurate character of these simplifications has been demonstrated, as briefly shown here below.

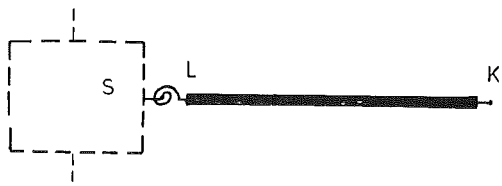

(a) Actual "beam + connection + sheared web panel" modelling

(b) Simplified "beam + joint" modelling (recommended in Eurocode 3)

Figure 5 Joint modelling

2.1.2 Validation of the simplified modelling and idealization

The non-linear behaviour of the rotational spring which characterizes the joint response cannot be accounted for in the design practice; the corresponding moment-rotation curve has consequently to be idealized. For class 1 joints, one of the most simple idealizations to which it may be referred to is the elastic-perfectly plastic one (Figure 2.a). This idealization has the advantage to be quite similar to that used traditionally for beam and column sections subjected to bending.

The moment corresponding to the yield plateau is the joint design moment M_{Rd} defined in Appendix 1. The values of the idealized constant stiffness S_j to be used for joints with end-plate and flange cleated connections are given in Eurocode 3 Annex J.

In [2], the structural response till collapse for six rectangular frames with different numbers of bays, storeys, connection type, loading, ... has been simulated by means of the geometrically and materially non-linear finite element program FINELG developed at the University of Liège by assuming successively that :

- the non-linear behaviour of the connections and of the sheared column web panels is modelled separately ("exact" simulation);
- the deformability of the connections and of the column web panels is concentrated into rotational springs acting at the beam-to-column intersection and characterized by bi-linear idealized laws.

From the comparison of these results [2], the safe and rather accurate character, at the global frame level, of the joint simplified modelling and bi-linearization has been demonstrated.

2.2 Local aspects

In Eurocode 3, when the design resistance M_{Rd} of a joint is reached, then a plastic hinge occurs and rotates as long as the maximum rotation capacity is not exceeded. In reality, the moment in the joint increases beyond M_{Rd}, because of the actual post-limit stiffness of the joint. This overloading of the joint is not of particular importance as long as the joint

behaves in a ductile way. It has so to be ensured that no brittle failure can occur in bolts and welds because of the joint overloading. The related provisions which have been included in Eurocode 3 Annex J by Weynand (University of Aachen), Steenhuis (TNO Delft) and ourself are described hereafter.

2.2.1 Weld design

In Eurocode 3 Annex J, welds have to be designed so as to carry a bending moment equal to [5] :

$$min\ (\gamma M_{Rd}\ ;\ M_{pl,Rd})$$

with :

$M_{pl,Rd}$ = design plastic moment resistance of the connected member (for a class 1 or 2 section)

γ = 1,4 for braced frames

= 1,7 for unbraced frames.

This design rule was already included in Annex J before its recent revision.

The requirements for unbraced frames are more severe than those for braced frames. This results from the higher need for rotation capacity to form a plastic mechanism in unbraced frames, and therefore from the higher "post-limit" moments reached in the joints.

2.2.2 Bolt design

Bolts are used to connect plates together. When these plates are subjected to transverse tension forces, the bolts work in tension.

In Eurocode 3 Annex J, three different failure modes are identified for such bolt-plate assemblies (see Appendix 3 for details). They are illustrated in Figure 6 :

- ***Mode 1 failure*** : in the case of thin plates and strong bolts, a plastic mechanism forms in the plate. This failure mode is very ductile and involve no failure of the bolts (Figure 6.a).

- ***Mode 3 failure*** : in the case of thick plates and weak bolts, no prying effects develop; the tensile force is simply carried over by the bolts until they reach failure (Figure 6.c). This brittle failure mode has to be avoided.

- ***Mode 2 failure*** : this intermediate failure mode involves some yielding in the plates before the bolts subjected to prying forces fail in tension (Figure 6.b).

As explained in Appendix 1, the term "failure" in Eurocode 3 does not relate to the actual failure mode, but to a sort of "design failure".

The F-Δ deformability curves corresponding to each of these failure modes are reported in Figure 7. When Mode 1 is predominant, the post-limit deformability is known to be quite big so a brittle collapse in the bolts is not likely to occur (Figure 7.a).

If Mode 3 is reached, no post-limit deformability exists and no plastic hinge has to be accepted in the joint (Figure 7.c). In practice, when such a situation occurs, the geometry of the joint has to be changed so to modify the failure mode.

In the case of Mode 2, the post-limit deformability varies from one joint to another, depending on its geometry. For rather thin plates, Mode 2 failure is quite close to Mode 1 and the actual bolt failure has not to be expected before a large post-limit deformability occurs (Figure 7.b.1). For rather thick plates, Mode 2 is close to Mode 3 and a brittle failure of the bolts in tension is quickly obtained if F_{Rd} (M_{Rd} in case of a whole joint) is exceeded (Figure 7.b.2).

In Annex J, provisions are given to avoid brittle failure resulting from joint overloading. These are commented hereafter.

Let us progressively increase the moment acting on a joint with an end-plate connection (see Section 3.2.3 of the present thesis). At the beginning, the forces distribute elastically between the different bolt-rows, according to their respective elastic stiffness, until the design resistance in one first bolt-row is reached. If the moment is increased beyond this maximum elastic design joint resistance, then plastic redistributions of internal forces in the joint occurs. This requires, for the already yielded components (those which have reached their own design resistance F_{Rd}), a sufficient deformation capacity. This means that locally, at the level of these bolt-rows, post-limit effects develop. If no brittle failure occurs, i.e. if, at the level of each bolt-row, a sufficient deformation capacity is available, a full plastic distribution takes place in the joint; the design moment M_{Rd} corresponds, in this case, to the full plastic resistance of the joint.

In Annex J, a criteria is given so as to check the sufficient deformation capacity at the level of each bolt-row. If the criteria is satisfied, the plastic redistribution of the internal forces can progress further. By similarity with beam and column sections, the joint is known to be "class 1" or "class 2". If it is not the case, the plastic redistribution has to be stopped and the moment resistance reached when the insufficient deformation is detected has to be considered as the maximum design resistance of the joint. The joint is then classified as "class 3".

The criteria is the following :

"The deformation capacity at the level of a bolt-row is sufficient as long as the corresponding design resistance F_{Rd} is lower or equal to 1,9 $B_{t,Rd}$, where $B_{t,Rd}$ is the design resistance of a bolt in tension".

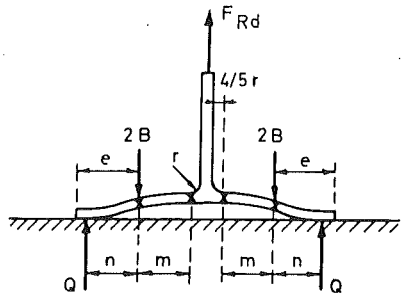

(a) Mode 1 collapse

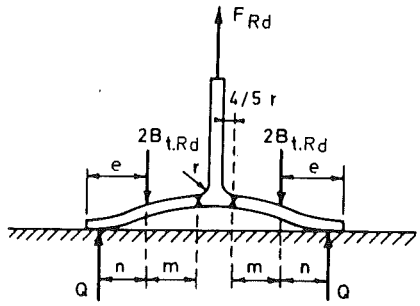

(b) Mode 2 collapse

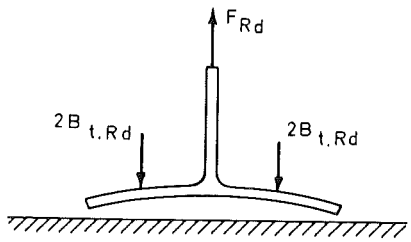

(c) Mode 3 collapse

Figure 6 Different failure collapse modes in a bolt-plate assembly

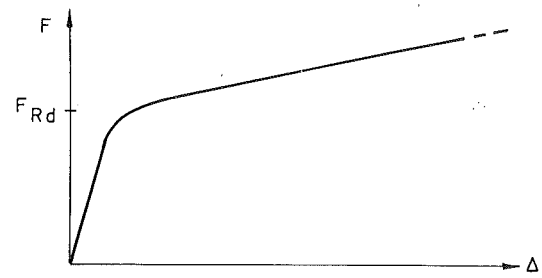

(a) Full ductile behaviour

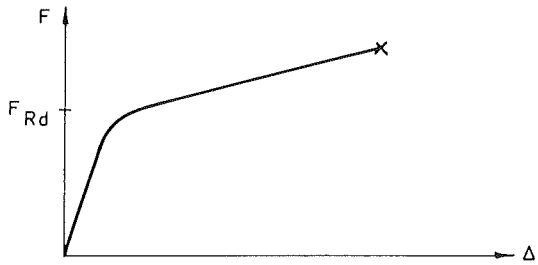

(b1) Good but limited ductility

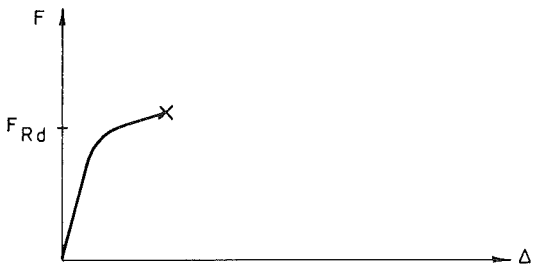

(b2) Really limited ductility

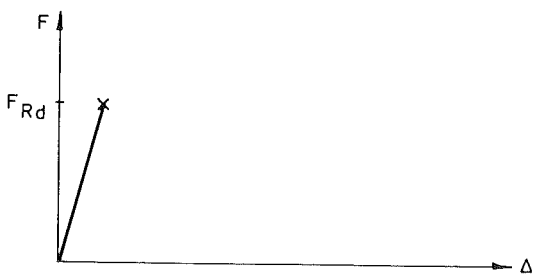

(c) Brittle behaviour

Figure 7 Deformability curves for bolt-plate assemblies

This criteria, the background of which is given in Appendix 3, applies to bolt-rows with two bolts. Its physical meaning is the following: when Mode 3 dominates, F_{Rd} is equal to $2B_{t.Rd}$ and no deformation capacity is available. When Mode 1 is predominant, F_{Rd} is low compared to $2B_{t.Rd}$ and a good deformation capacity is available. For Mode 2 failure, the deformation capacity is rather good, except when the failure mode is close to Mode 3, i.e. when F_{Rd} is close to $2B_{t.Rd}$. The boundary "$1{,}9\ B_{t.Rd}$" just gives the limit beyond which the deformation capacity is not sufficient to ensure that no brittle failure occurs during the plastic redistribution of the internal forces in the joint.

For "class 1" or "class 2" joints, M_{Rd} is reached by full plastic redistribution of the internal forces. According to Eurocode 3, no further increase of the resistance is possible and the concept of plastic hinge is introduced. This hinge only rotates as long as some rotation capacity is available. Provisions have therefore been included in Annex J so as to check whether the rotation capacity is sufficient or not, i.e. whether the actual post-limit stiffness is not likely to lead to a brittle failure of the bolts in tension. This is achieved by limiting the thickness t of the connected plates to :

$$t \leq 0{,}36\, d \sqrt{f_{ub}/f_y}$$

where: d = bolt diameter

f_{ub} = yield stress of the bolt

f_y = yield stress of the plate.

This condition has to be fulfilled at least by one of the connected plate. It ensures that Mode 1 is governing and that no brittle failure is therefore likely to occur. Its derivation is given in Appendix 3.

The development of plastic hinges in joints which would not fulfil this requirement has to be prevented.

Finally, overstrength effects can also lead to brittle failure in the joints. These ones result from the difference between the actual mechanical properties of the steel joint components and of the beam and column sections, on one hand, and the design values taken into consideration in the code (characteristic values and γ partial safety factors), on the other hand. As a consequence, situations can occur in which a hinge forms, in the real structure, in the joint while, when comparing the *design* resistances of the beam and of the joint, it was expected to form in the beam .

That is why, in Eurocode 3, the rotation capacity of "full strength" joints - joints, the design resistance of which is higher than that of the connected members - has to be checked, as long as their design resistance is not higher than 1,2 times the design resistance of the weakest of the connected members. Beyond this boundary, the hinge is assumed to form in one of the connected members, but no more in the joint.

3. FINAL REMARK AND CONCLUSION

When yielding, structural joints develop strain-hardening under increasing bending moments. In some of them, high membrane effects appear simultaneously, what results in a rather high "post-limit" stiffness.

In Eurocode 3, this post-limit stiffness is neglected for global frame analysis and design as well as for local joint design, but provisions are given to avoid brittle failures to appear in welds and bolts. These brittle failures could result from the overloading of the joints - beyond M_{rd} - because of this actual post-limit stiffness.

The provisions have been validated for joints developing "normal" post-limit stiffness, but not for joints developing a high post-limit stiffness as minor-axis beam-to-column joints. This work is now in progress in the frame of the activities of the COST C1 Working Group on "Steel and Composite"; a preliminary study is already available in [4].

As a last comment, it has to be mention that joint overloading is not only linked to post-limit effects but can also results from "overstrength effects" (the fact that the *design* resistances are less than the *actual* ones can lead to an underestimation of the actual bending moments acting in the joints). These ones are due to the difference between the *actual* mechanical properties of steel joint components and beam or column sections and the *design* values taken into consideration for design (characteristic values and γ factors).

The risk of brittle failure by overstrength effects should is also covered by the provisions given in Eurocode 3.

4. REFERENCES

[1] EUROCODE 3, ENV-1993-1-1, Revised Annex J, Design of Steel Structures.

CEN, European Committee for Standardization, Document CEN/TC250/SC3 - N419E, Brussels, June 1994.

[2] Jaspart, J.P.

Etude de la semi-rigidité des noeuds poutre-colonne et son influence sur la résistance et la stabilité des ossatures en acier.

Ph.D.Thesis, University of Liège, Belgium, 1991.

[3] Jaspart, J.P. and Maquoi, R.

Prediction of the semi-rigid and partial-strength properties of structural joints.

COST C1 WG2 document C1/WD2/94-11, November 1994.

[4] Vandegans, D. and Jaspart, J.P.

Influence if the post-limit stiffness of joints on the frame behaviour.

COST C1 WG2 C1/WD2/95-03 document. April 1996.

[5] Zoetemeijer, P.

Summary of the researches on bolted beam-to-column connections.

Report 6-85-7, TH Delft, The Netherlands, November 1983.

[6] Janss, J., Jaspart, J.P. and Maquoi, R.

Strength and behaviour of in-plane minor axis joints and 3-D joints.

Proceedings of a state-of-the-art Workshop on Connections and the Behaviour, Strength and Design of Steel Structures, Cachan, France, May 25-27, 1997.

[7] Vandegans, D.

Liaison entre poutres métalliques et colonnes en profils creux remplis de béton basée sur la technique du goujonnage (goujons filetés).

Research report MT 193, CRIF, Belgium, October 1995.

APPENDIX 3

DESIGN STIFFNESS AND RESISTANCE PROPERTIES OF BOLTED JOINTS MAY BE SIGNIFICANTLY INCREASED BY THE ADDITIONAL CONSIDERATION OF THE BOLT HEAD SIZE AND THE BOLT PRELOADING

1. INTRODUCTION

According to the component method - which is described in Chapter 2 - any structural joint is considered as a set of basic individual components.

When deriving the mechanical properties of a joint, the list of active components has first to be established. In a second step, the mechanical properties of the components in compression, tension or shear are evaluated. Finally, the assembly of the components is achieved through an appropriate distribution of the external forces into so-called internal forces acting on the components. When distributing the forces, it is required to fulfil equilibrium and never exceed the proper resistance neither the deformation capacity of the constitutive components.

Amongst the available components, some appear as plates subjected to transverse forces : column flanges in bending, end-plates in bending and flange cleats in bending. These are represented in Figure 1.

In the present appendix, the evaluation of the resistance and stiffness properties as well as the deformation capacity of the components is first discussed. The beneficial influence of the bolt preloading on the stiffness and resistance properties is then demonstrated. Lastly simplified formulae for an easy and simple evaluation of these characteristics are presented.

Some of the latter have been introduced in the revised Annex J of Eurocode 3 on "Joints in Steel Building Frames" [13].

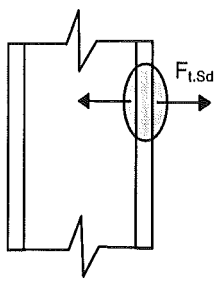

Column flange in bending

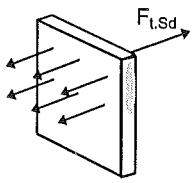

End-plate in bending

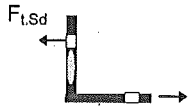

Flange cleat in bending

Figure 1 Plated components

2. "PLATE" AND "T-STUB" APPROACHES

Two main approaches respectively termed "plate model" and "T-stub model" are referred to in the literature for the evaluation of the resistance of plated components subjected to transverse bolt forces. (see Table 1).

Model	Column flange	End-plate	Both
Plate	Packer-Morris [14] Zoetemeijer [3]	Wittaker-Walpole [15] Zanon [16] Surtees-Mann [17] Zoetemeijer [3]	Zoetemeijer [3] Eurocode 3 [13] Packer-Morris [14]
T-stub	Zoetemeijer [3] Eurocode 3 [13]	Zoetemeijer [3] Packer-Morris [14] Kato-McGuire [18] Agerskov [19] Eurocode 3 [13]	

Table 1 "Plate" and "T-stub" models for column flanges and end-plates in bending

The first one, the "plate model", considers the component as it is - i.e. as a plate - and formulae for resistance evaluation are derived accordingly. The actual geometry of the component, which varies from one component to another, has to be taken into consideration in an appropriate way; this leads to the following conclusions :

- the formulae for resistance varies from one component to another;
- the complexity of the plate theories are such that the formulae are rather complicated and therefore not suitable for practical applications.

The T-stub idealization, on the other hand, consists in substituting to the tensile part of the connection T-stub sections of appropriate effective length ℓ_{eff}, connected by their flange onto a presumably infinitely rigid foundation and subject to a uniformly distributed force acting in the web plate (Figure 2 and Figure 3).

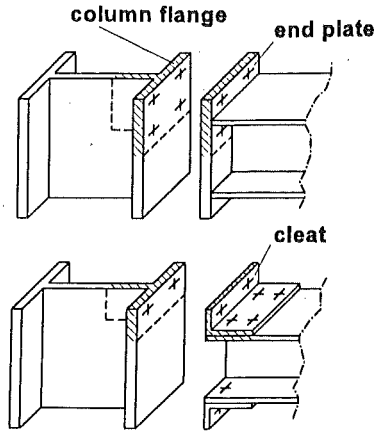

Figure 2 T-stub idealizations

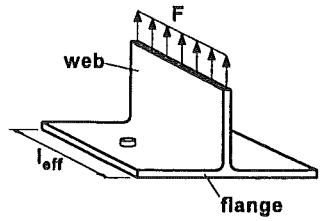

Figure 3 T-stub on rigid foundation

In comparison with the plate approach, the T-stub one is easy to use and allows to cover all the plated components with the same set of formulae. Furthermore, the T-stub concept may also be referred to for stiffness calculations as shown [1] and [2].

This explains why the T-stub concept appears now as the standard approach for plated components and is followed in all the modern characterization procedures for components, and in particular in Eurocode 3.

A particular aspect of the T-stub calculation is the influence of the bolt preloading on the force-displacement response (F-Δ curve), as pointed out in Figure 4 which relates to tests recently performed in Liège on similar T-stubs connected respectively by means of preloaded and non-preloaded bolts. Tests show that :

- the bolt preloading has a significative influence on the initial stiffness and on the pseudo-plastic resistance of the connection and;
- a non significative influence on the ultimate resistance because of the complete loss of preloading between the connected flanges at that load level.

In the next pages, the evaluation of the resistance and stiffness properties of the T-stub are discussed and proposals for inclusion of the bolt preloading effects are presented.

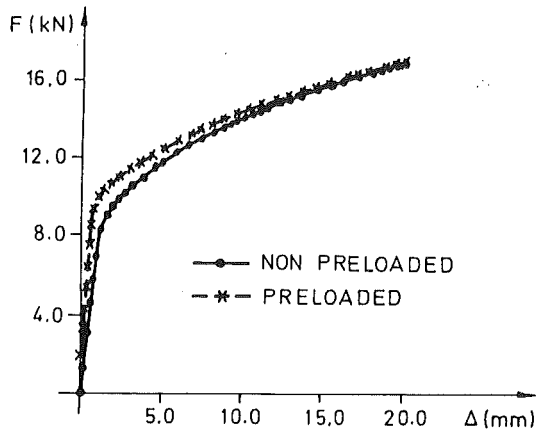

Figure 4 Effect of bolt preloading on the T-stub response

3. DESIGN RESISTANCE OF PLATED COMPONENTS

3.1 Basic formulae of Eurocode 3

The T-stub approach for resistance, as it is described in Eurocode 3, has been first introduced by Zoetemeijer [3] for unstiffened column flanges. It has been then improved [4] so as to cover other plate configurations such as stiffened column flanges and end-plates. In [1], it is also shown how to apply the concept to flange cleats in bending.

In plated components, three different failure modes may be identified (Figure 5):

a) Bolt fracture without prying forces, as a result of a very large stiffness of the plate (Mode 3)

b) Onset of a yield lines mechanism in the plate before the strength of the bolts is exhausted (Mode 1)

c) Mixed failure involving yield lines - but not a full plastic mechanism - in the plate and exhaustion of the bolt strength (Mode 2).

The same failure modes may be observed in the actual plated components (Figure 5.a) and in the flange of the corresponding idealized T-stub (Figure 5.b). As soon as the effective length ℓ_{eff} of the idealized T-stubs is chosen such that the failure modes and loads of the actual plate and the T-stub flange are similar, the T-stub calculation can therefore be substituted to that of the actual plate.

Actual component Equivalent T-stub Moment diagram

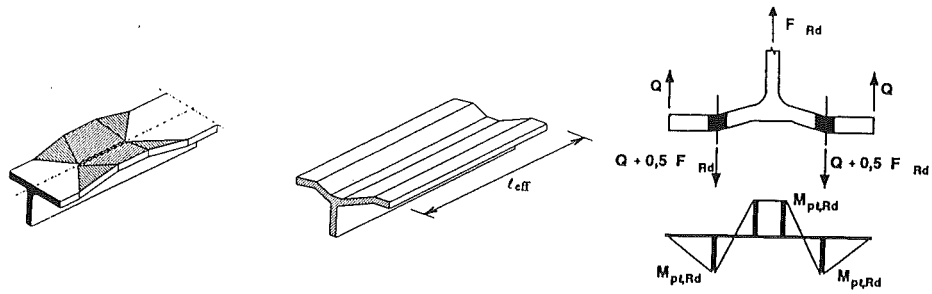

Mode 1 : Complete yielding of the flange

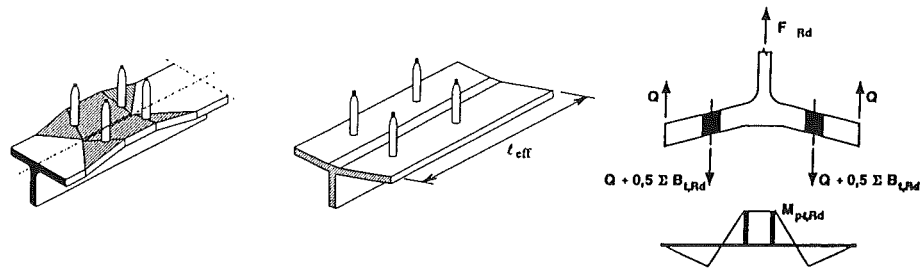

Mode 2 : Bolt fracture with yielding of the flange

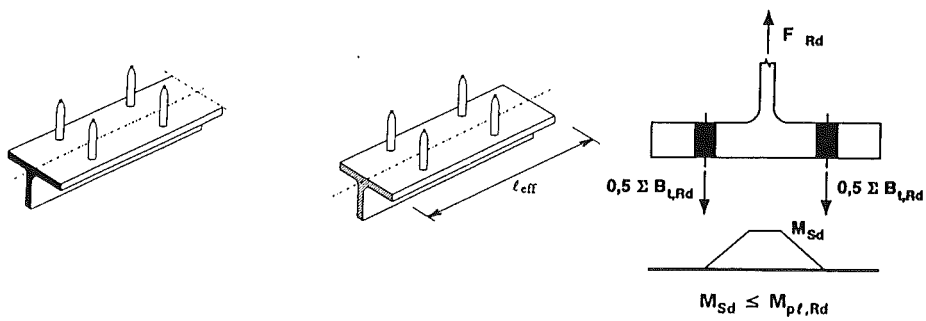

Mode 3 : Bolt fracture

(a) Actual plate (b) Equivalent T-stub

Figure 5 Failure modes for plated components

In Eurocode 3, the design resistance of a T-stub flange of effective length ℓ_{eff} is derived as follows for each failure mode :

Mode 3 :bolt fracture (Figure 6.a)

$$F_{Rd,3} = \Sigma B_{t,Rd} \tag{1}$$

Mode 1 :plastic mechanism (Figure 6.b)

$$F_{Rd,1} = \frac{4\ell_{eff} m_{pl,Rd}}{m} \tag{2}$$

Mode 2 :mixed failure (Figure 6.c)

$$F_{Rd,2} = \frac{2\ell_{eff} m_{pl,Rd} + \Sigma B_{t,Rd} n}{m+n} \tag{3}$$

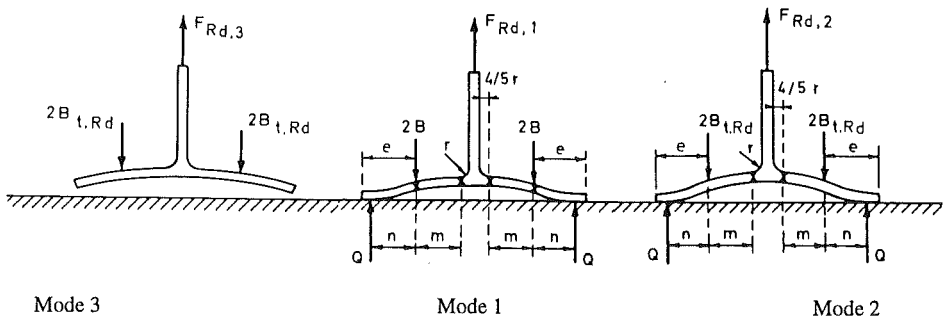

Figure 6 Failure modes in a T-stub

In these expressions :

$m_{pl,Rd}$ is the plastic moment of the T-stub flange per unit length ($\frac{1}{4} t^2 f_y / \gamma_{M0}$) with t = flange thickness, f_y = yield stress of the flange, γ_{M0} = partial safety factor)

m and e are geometrical characteristics defined in Figure 6

$\Sigma B_{Bt,Rd}$ is the sum of the design resistances $B_{t,Rd}$ of the bolts connecting the T-stub to the foundation ($B_{tRd} = 0{,}9\ A_s f_{ub}/\gamma_{Mb}$ where A_s is the tensile stress area of the bolts, f_{ub} the ultimate stress of the bolts and γ_{Mb} a partial safety factor)

n designates the place where the prying force Q is assumed to be applied, as shown in Figure 6 ($n = e$, but its value is limited to 1,25 m).

ℓ_{eff} is derived at the smallest value of the effective lengths corresponding to all the possible yield lines mechanisms in the specific T-stub flange being considered.

The design strength F_{Rd} of the T-stub is derived as the smallest value got from expressions (1) to (3) :

$$F_{Rd} = min(F_{Rd,1}, F_{Rd,2}, F_{Rd,3}) \qquad (4)$$

In [1], the non-significative influence of the possible shear-axial-bending stress interactions in the yield lines on the design capacity of T-stub flanges has been shown.

This calculation procedure recommended first by Zoetemeijer has been refined when revising the Annex J of Eurocode 3.

Eurocode 3 distinguishes now between so-called circular and non-circular yield lines mechanisms in T-stub flanges (see Figure 7.a). These differ by their shape and lead to specific values of T-stub effective lengths noted respectively $\ell_{eff,cp}$ and $\ell_{eff,nc}$. But the main difference between circular and non-circular patterns is linked to the development or not of prying forces between the T-stub flange and the rigid foundation : circular patterns form without any development of prying forces Q, and the reverse happens for non-circular ones.

The direct impact on the different possible failure modes is as follows :

Mode 1 : the presence or not of prying forces do not alter the failure mode which is linked in both cases to the development of a complete yield mechanism in the plate. Formula (2) applies therefore to circular and non-circular yield patterns.

Mode 2 : the bolt fracture clearly results here from the over-loading of the bolts in tension because of prying effects; therefore Mode 2 only occurs in the case of non-circular yield lines patterns.

Mode 3 : this mode does not involve any yielding in the flange and applies therefore to any T-stub.

As a conclusion, the calculation procedure differs according to the yield line mechanisms developing in the T-stub flange (Figure 7.b) :

$$F_{Rd} = min(F_{Rd,1}; F_{Rd,3}) \qquad \text{for circular patterns} \qquad (5.a)$$

$$F_{Rd} = min(F_{Rd,1}; F_{Rd,2}; F_{Rd,3}) \qquad \text{for non-circular patterns} \qquad (5.b)$$

In Annex J, the procedure is expressed in a more general way. All the possible yield line patterns are considered through recommended values of effective lengths grouped into two categories : circular and non-circular ones. The minimum values of the effective lengths - respectively termed $\ell_{eff,cp}$ and $\ell_{eff,nc}$ - are therefore selected for category. The failure load is then derived, by means of Formula (4), by considering successively all the three possible failure modes, but with specific values of the effective length :

Mode 1 : $\ell_{eff,1} = min(\ell_{eff,cp}; \ell_{eff,nc})$ (6.a)

Mode 2 : $\ell_{eff,2} = \ell_{eff,nc}$ (6.b)

Mode 3 : - (6.c)

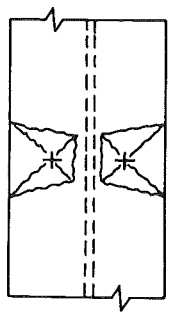

Circular pattern ($l_{eff,cp}$)

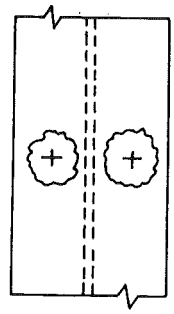

Non-circular patterns ($l_{eff,nc}$)

(a) Different yield line patterns

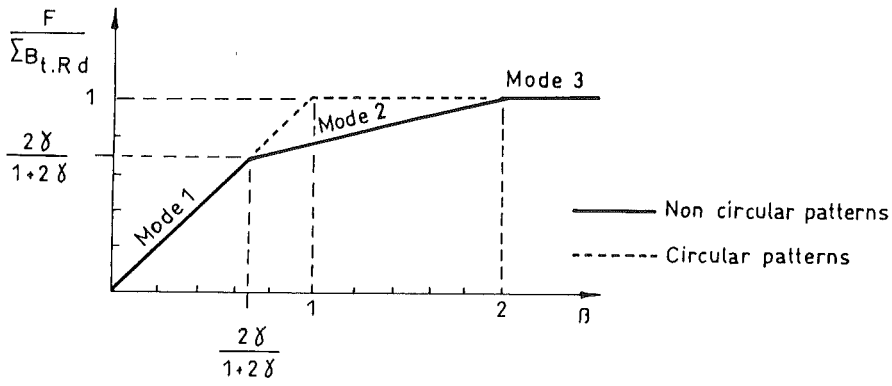

$\gamma = n/m$ $\qquad \beta = \dfrac{4 M_{pl.Rd}}{m \Sigma B_{t.Rd}} = \dfrac{l_{eff.} t^2 f_y / \gamma M0}{m \Sigma B_{t.Rd}}$

(b) Design resistance

Figure 7 T-stub resistance according revised Annex J

3.2 Improvements to the basic T-stub model of Eurocode 3

On the basis of comparisons between test results and Eurocode 3 prediction model for joint characterization - as those shown in section 3.3. -, the quite valuable character of the T-stub approach has been demonstrated. Its accuracy has be seen as quite good when the resistance is governed by failure modes 2 and 3. The formulae for failure mode 1, on the other hand, has been seen quite conservative, and sometimes too conservative, when a plastic mechanism forms in the T-stub flange [1].

The question raised whether refinements could be brought to the T-stub model of Eurocode 3 with the result that the amended model would provide a higher resistance for failure mode 1 without altering significantly the accuracy regarding both failure modes 2 and 3.

We have recently made an attempt in this respect. In all the existing methods, it shall be noticed that the forces in the bolts are always idealized as point loads. Thus, it is never explicitly accounted for the actual sizes of the bolts and washers, on the one hand, and on the degree of bolt preloading, on the other hand. Care taken of the both aspects should influence the location of some of the yield lines forming the plastic mechanism as well as the contribution of the external loads to the virtual work associated to this mechanism.

In the T-stub model, the plastic mechanism is composed of parallel straight yield lines which develop in the flange of the T-section. Two of them are always located at the toe of the fillets. The two others are located in the vicinity of the bolt-rows. In some models they coincide with the axes of the bolts [3, 4]; that means that the bolt size is fully disregarded and that the load is applied at the axis of the bolts (Figure 8.a). In other models, bolts and washers are assumed so stiff that the yield lines are forced to develop at the inner extremity of the bolt/washer diameter [5] , where the bolt load is also assumed to be applied (Figure 8.c). None of these models is in very fair agreement with experimental observations. Indeed the lines of maximum curvature are actually not straight but slightly curled and their pattern in the close vicinity of the bolts is found to depend on the stiffness of the bolts and on the degree of bolt preloading (Figure 8.b)). For practical purposes, one cannot imagine to account for such a complex actual pattern. It must be noticed that, for well proportioned connections, the yield lines are not far from complying with Zoetemeijer's assumption; it is therefore justified to refer to the latter for what regards the location of the yield lines.

In the calculation method we suggest, the bolt size is taken into consideration at another level : it is assumed that the bolt load exerted onto the T-stub flange is uniformly distributed over a certain length d_w located symmetrically with respect to the bolt axis (Figure 8.b); d_w designates the diameter of the bolt head/screw or washer. Of course, in these conditions, the location of the yield lines does no more coincide necessarily with the section of maximum bending moment, what results in a non-compliance with the fundamental theorems of plastic design; we are however of the opinion that the error remains sufficiently small to be acceptable. Accordingly half of the force in the bolts develops a negative external work when the plastic mechanism forms with the result of an expected higher T-stub capacity in comparison with Eurocode 3 model. For sake of simplicity, the bolt load $2B$ is substituted

by two equal statically equivalent load, B acting at a distance $\pm e_w = 0.25\ d_w$ from the bolt axis (Figure 9).

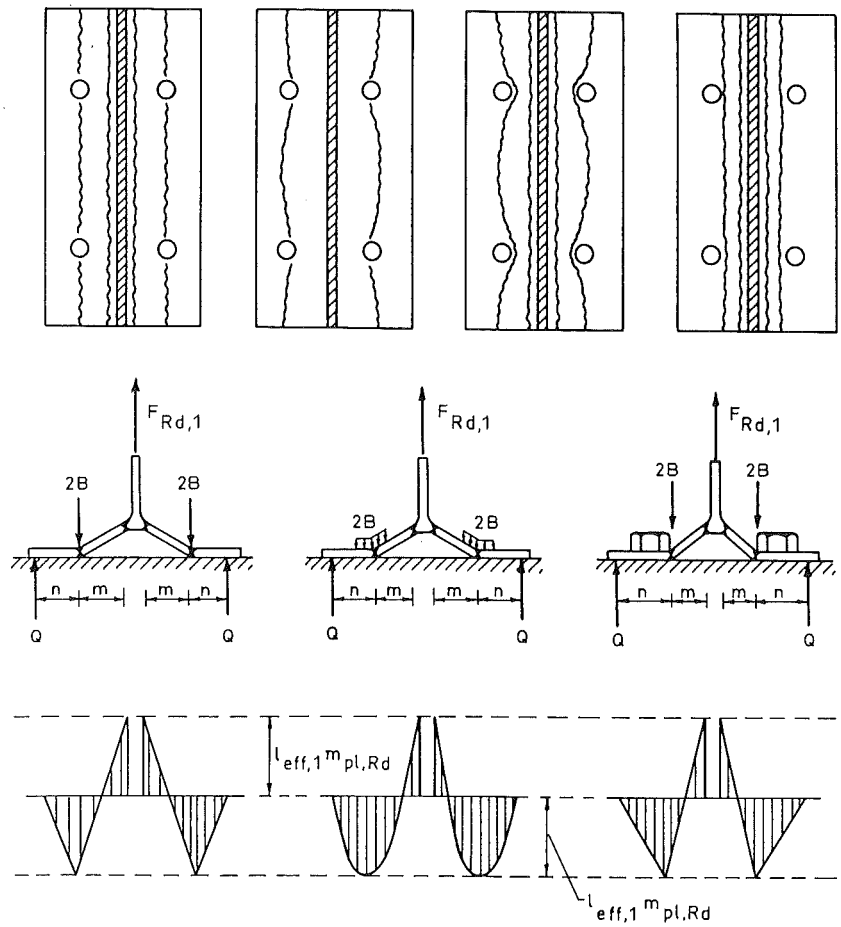

(a) Bolts fully flexible in bending (b) Intermediate solution (c) Bolts infinitely stiff in bending

Figure 8 Influence of bolt dimensions on the yield line mechanism

By applying the principle of virtual work to above plastic mechanism, on the one hand, and the equations of equilibrium, on the other hand, the limiting force $F_{Rd,1}$ associated to a failure by onset of a plastic mechanism may be derived :

$$F_{Rd,1} = \frac{(8n - 2e_w)\ell_{eff,1} m_{pl,Rd}}{[2mn - e_w(m+n)]} \tag{7}$$

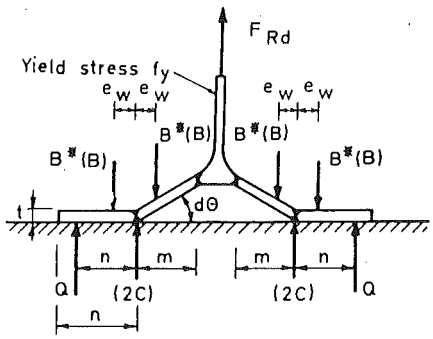

Figure 9 Forces acting on a T-stub

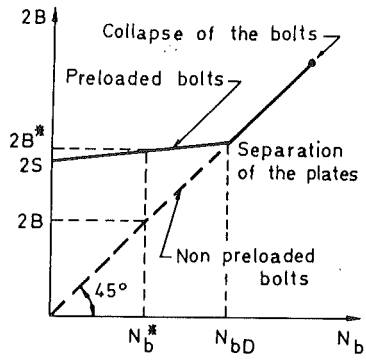

Figure 10 Bolt force versus external load

Of course, equ. (5) confines itself to Zoetemeijer's one formulae when distance e_w is vanishing.

What is said above is not explicitly influenced by the degree of bolt preloading. Actually the force in the preloaded bolts of an elementary bolt assembly subject to an increasing external load N_b (parallel to the bolt axis) evolves according to Figure 10. First, the bolt tension increases is a reduced proportion of the external load because of the compensating effect of the reduction in plate compression $2C$. When the latter becomes equal and opposite to the initial contraction of the plate ($N_b = N_{bD}$), the plates start to separate and the system becomes statically determinate. At any higher load, the bolts experience the whole load N_b. Separation occurs at :

$$N_{bD} = 2S/K^* \tag{8}$$

where S is the preloading force per bolt and $K^* = 1/(1 + 1/\xi)$. The factor $\xi = A_t/A_b$ is the ratio between the axial stiffness of the effective plate compression area A_t and the resisting bolt cross-sectional area A_b; it is taken as 5 as an average value [6]. Proceeding as before with attention duly paid to the effect of bolt preloading yields the amended expression of the limiting force $F^*_{Rd,1}$:

$$F^*_{Rd,1} = \frac{\left\{\left[8n - 2(1-K^*)e_w\right]\ell_{eff,1}m_{pl,Rd} + 4ne_wS\right\}}{\left[2mn - e_w(1-K^*)(m+n)\right]} \tag{9}$$

under the reservation that :

$$2B \equiv (F^*_{Rd,1}n + 2\ell_{eff,1}m_{pl,Rd})/(2n - e_w) \not> N_{bD} \tag{10}$$

because equ. (9) is valid in the range prior to plate separation. Should condition (10) not be fulfilled, then reference is made to (9) where $K^* = 0$, what results in $F^*_{Rd,1} = F_{Rd,1}$ with $F_{Rd,1}$ given by equ. (7).

The limiting force according to (9), subordinated to the additional check (10), could constitute a refinement of the relevant Eurocode 3 design rule for Mode 1 failure. It is quite clear that above bolt effects do not at all alter the capacities associated respectively to the two other collapse modes of the T-stub.

3.3 Comparison of the refined model with test results for joints with end-plate connections

Only few test specimens have been sufficiently instrumented to allow for a valuable comparison. It is referred to results obtained on isolated end-plates in Milano [7] and on full joints in Liège [1] and Delft [3].

Predictions according to our proposal are superimposed in Figure 11.a and b to a diagram established elsewhere [8] for isolated end-plates; those relative to full joints are listed in Table 2.

It may be concluded to a very significative improvement of the design rules and to a better accuracy. The refined model is still somewhat too conservative in a range where the bolts are not well proportioned to the stiffness of the plates (see especially the Italian tests with a end-plate thickness of 12 and 15 mm); then the conditions become close to Kishi's assumption with the result of an increase in the corresponding capacity. Such a range of not well proportioned connections will probably be met only exceptionally because not economical at first sight; anyway the approach provides conservative results in such cases.

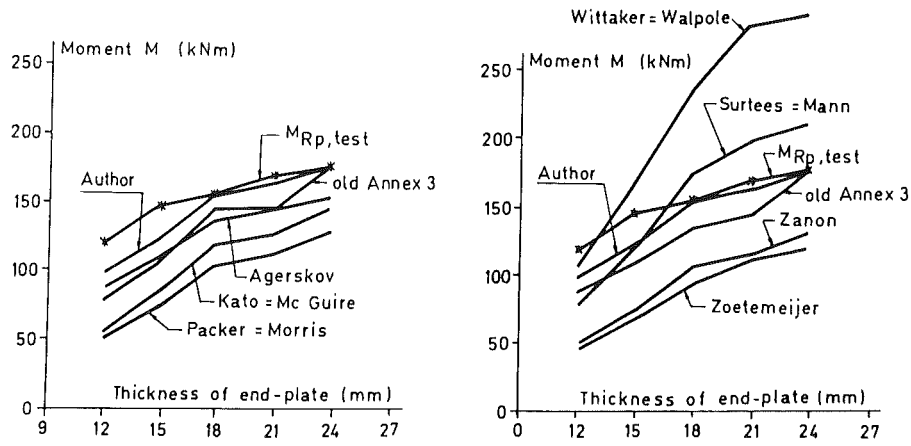

Figure 11 Test-model comparisons for isolated end-plates (T-stub models).

Test	Laboratory	$M_{Rp,model}/M_{Rp,test}$	
		Author	Packer-Morris
01	Liège	0.98	1.10
04	Liège	1.04	1.15
07	Liège	0.98	1.08
014	Liège	1.01	0.91
T9	Delft	1.02	0.77
T20	Delft	1.08	0.90

Table 2 Test-model comparisons for joints with end-plate connections

3.4 Application to joints with flange cleated connections

The critical part of a flange cleated connection is usually the cleat in bending and the adjacent zone (bolts in tension and column flange in bending). Mainly two methods for assessing the pseudo-plastic capacity of the tensile zone are available [11], [5]. Both have been used for a comparison with fully instrumented test results performed in Trento [9] on isolated cleats and in Liège [1], Sheffield [10] and Hamburg [11] on joints with flange cleated connections. It results that Kishi's method is largely unconservative and Hotz's one much too conservative. The large discrepancy is, to our opinion, due to specific aspects which are not properly accounted for by both methods [1]. It follows from experimental observations that :

- The failure of a flange cleated connection by formation of a plastic mechanism involves a three-yield lines mechanism (two in the cleat in bending, one in the cleat located in the compressive zone).

- The initial clearance between the beam end and the column flange is likely to change the location of one yield line in the cleat in bending; the latter always develops at the toe the cleat fillet, at one time in the vertical leg, at one time in the horizontal leg.

In addition, the sole way to define the experimental plastic capacity of a cleated connection is not likely to correspond to the lowest strength of the connection components [1]. Let us just mention that the degree of bolt preloading and the onset of an appreciable membrane action are the main reasons.

In [1], we have developed a fully original approach on a similar basis than that used for end-plate connections. It accounts for the more accurate location of the yield lines, the sizes of the bolts/or washers, the bolt preloading and the plastic mechanism of the connection in its whole. As a result, a set of design formulae have been suggested; they cover all the

possible collapse modes : bolt fracture, mixed plastic mechanism in the whole connection, and yield line mechanism either in the cleats or in the column flange.

Test	Laboratory	$M_{Rp,model}/M_{Rp,test}$		
		Author	Kishi-Chen	Hotz
03	Liège	1,01	(-)	0,52
06	Liège	1,01	(-)	0,55
012	Liège	1,02	(-)	0,78
JT08	Sheffield	1,05	(-)	0,75
TT1(*)	Trento	0,86	1,40	0,42
TT2(*)	Trento	0,89	1,46	0,44
A	Hamburg	0,89/1,04	1,28/1,64	0,51/0,65
B	"	0,83/0,97	1,16/1,51	0,47/0,60
E	"	0,89/1,04	1,21/1,57	0,49/0,63
F	"	1,01/1,15	(-)	0,47/0,60
G	"	0,80/0,94	1,15/1,47	0,45/0,58
H	"	0,92/1,06	1,25/1,62	0,51/0,65
I	"	1,00/1,12	(-)	0,48/0,61

Table 3 Test-model comparisons for joints with flange cleated connections

(*) connection not well proportioned

(-) method not applicable

../.. extreme values because actual yield stress not measured.

The theoretical results computed in accordance with this new approach have been compared with test data (Table 3). It may be concluded that the method has a wide range of application and a very good accuracy.

3.5 Amendments introduced in Eurocode 3 Annex J

During the recent revision of Annex J of Eurocode 3, formula (7) which describes the Mode 1 failure as dependent on the actual bolt dimensions has been agreed for inclusion as an alternative to formula (2). On the other hand, the influence of the bolt preloading on the plastic resistance of the T-stub components has not been considered because of the extra complexity resulting from the use of formula (9) under condition (10).

As a result, the resistance properties of the T-stub components remain unchanged in Eurocode 3 whatever is the bolt preloading. The safe character of this assumption is demonstrated in Appendix 2 of the present thesis.

A cleat in bending being also considered as a T-stub (see Figure 12), formula (7) applies also in this case. The different location of the plastic hinges in the cleats according to the value of the gap between the beam end and the column flange has been pointed out in [1], as already said, and has therefore been taken into consideration in the revised Annex J. According to our proposal - based on previous studies reported in [1] -, the values of the m and e characteristics necessary for the evaluation of the T-stub resistance have been adopted as shown in Figure 13.

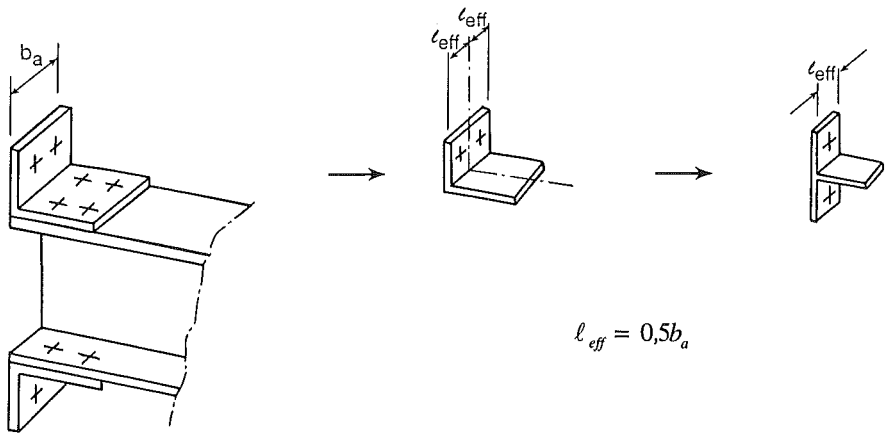

Figure 12 Effective length ℓ_{eff} of an angle flange cleat

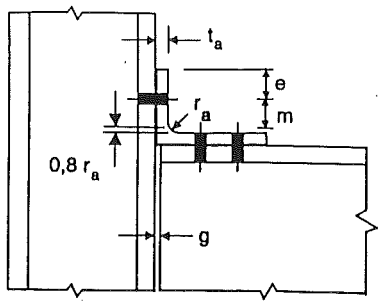

(a) Gap $g \leq 0{,}4\ t_a$ between the beam end and the column face

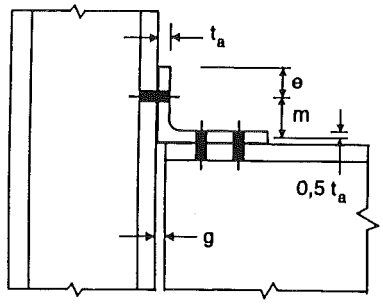

(b) Gap $g > 0{,}4\ t_a$ between the beam end and the column face

Notes :

- The number of bolt-rows connecting the cleat to the column flange is limited to one;
- The number of bolt-rows connecting the cleat to the beam flange is not limited;
- The length of the cleat may be different from both the width of the beam flange and the width of the column flange.

Figure 13 Dimensions *e* and *m* for a bolted flange cleat

4. INITIAL STIFFNESS OF PLATED COMPONENTS

4.1 Application of the T-stub approach

For plated components, it is also referred to the T-stub concept where, in the particular case of an end-plate connection, the column flange and the end-plate in bending are idealized as two T-stubs connected together (see Figure 14).

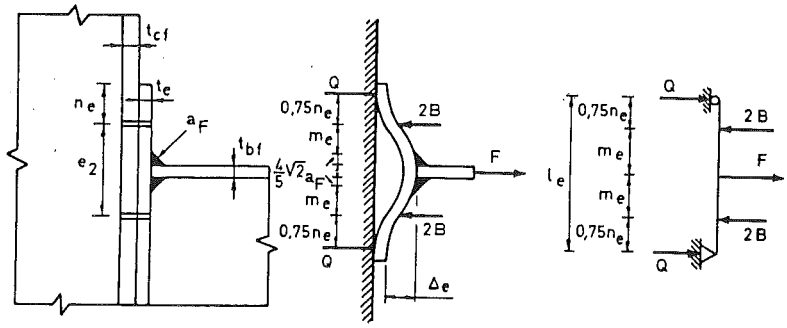

(a) End-plate (Δ_e)

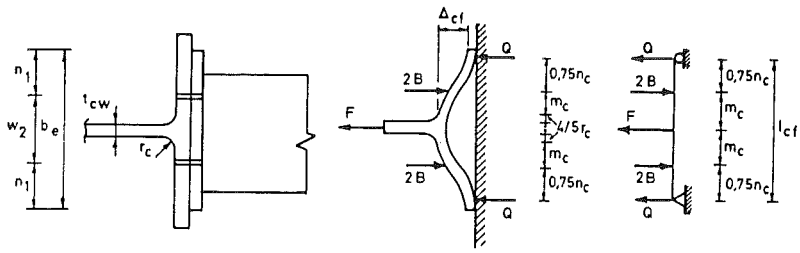

(b) Column flange (Δ_{cf})

Figure 14 End-plate and column flange deformability

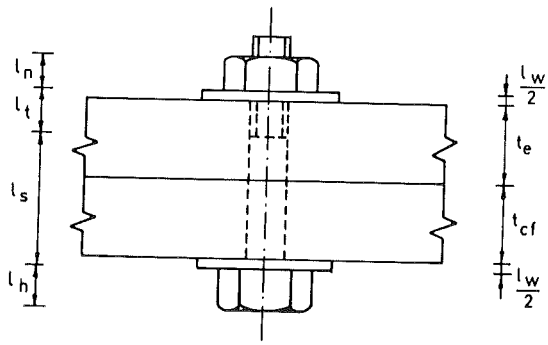

Figure 15 Bolt geometrical properties

For each of the two T-stubs, the tensile stiffness results from the elastic deformation of the T-stub flange in bending and of the bolts in tension. But the initial stiffness of each T-stub can not be evaluated independently. As a matter of fact, the bolts in tension belong to the two T-stubs and the compatibility between the respective deformabilities of the T-stub flanges and of the bolts has to be ensured :

$$\Delta_e^* + \Delta_{cf}^* = \Delta_b$$

where Δ_e^* is the deformation of the end-plate at the level of the bolts;

Δ_{cf}^* is the deformation of the column flange at the level of the bolts;

Δ_b is the elongation of the bolts.

In [1], we have proposed expressions providing the elastic initial stiffness of each T-stub; they allow the coupling effect between the T-stubs to be taken into consideration. These expressions differ from those given in the original publication of Yee and Melchers [2] for the two following reasons :

- some corrections have been brought to the original formulae proposed by Yee and Melchers; these corrections are given in [1];
- the location of the prying forces Q (see Figure 16.b) considered by Yee and Melchers is not optimum; several researches have shown that, in the elastic range of behaviour, the prying forces may be located closer to the bolts; we have referred to the proposal made by Douty and McGuire in [12] (see Figure 16.c).

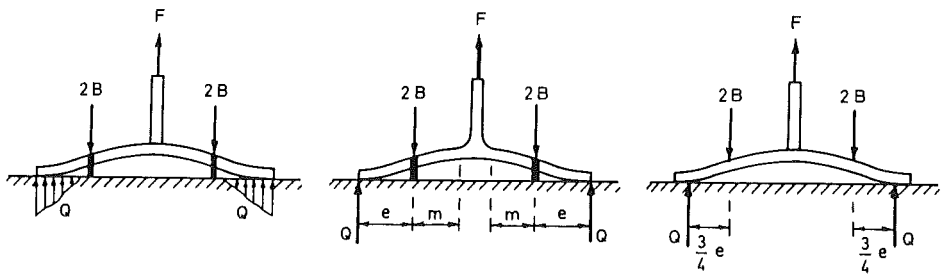

(a) Actual distribution

(b) Idealisation by Yee and Melchers

(c) Idealisation by Douty and McGuire

Figure 16 Location of the prying forces

When non-preloaded bolts are used, the elongation Δ_b (Figure 17) of the bolts simply results from the elongation of the bolt shank subjected to tension. On the contrary, when bolts are preloaded, tensile forces on the bolt-plate assembly result more in a decrease of the

compressive forces between the connected plates that in an increase of the bolt tensile force. The "decompression" stiffness of the plates is much higher than that of the bolts in tension.

- for non preloaded bolts :

$$\Delta_b = \frac{B}{EA_S}(k_1 + 2k_4) \tag{11}$$

- for preloaded bolts

$$\Delta_b = \frac{B(t_e + t_{cf})}{10EA_S}\frac{1}{1+\frac{k_3}{k_2}} \tag{12}$$

where (Figure 17) :

$$k_1 = \ell_s + 1{,}43\ell_t + 0{,}71\ell_n$$

$$k_2 = \ell_s + 1{,}43\ell_t + 0{,}91\ell_n + 0{,}4\ell_w$$

$$k_3^* = \frac{t_e + t_{cf}}{5}$$

$$k_4 = 0{,}1\ell_n + 0{,}2\ell_w$$

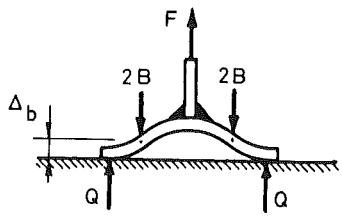

Figure 17 T-stub deformability

From these considerations, the elastic deformation of the two T-stubs may be derived :

$$\Delta_e = \frac{F}{Ek_{i,e}} \tag{13}$$

$$\Delta_{cf} = \frac{F}{Ek_{i,cf}} \tag{14}$$

where the stiffness coefficient $k_{i,e}$ and $k_{i,cf}$ are expressed as :

$$k_{i,cf} = \left[Z_{cf} \left(\frac{1}{8} - \frac{1}{4} q \alpha_{cf} \right) \right]^{-1} \tag{15.a}$$

$$k_{i,e} = \left[Z_{e} \left(\frac{1}{8} - \frac{1}{4} q \alpha_{e} \right) \right]^{-1} \tag{15.b}$$

For connections with non-preloaded bolts :

$$q = \frac{Z_e a_{e1} + Z_{cf} \alpha_{cf1}}{Z_e \alpha_{e2} + Z_{cf} \alpha_{cf2} + \dfrac{k_1 + 2k_4}{2A_S}} \tag{16.a}$$

For connections with preloaded bolts :

$$q = \frac{Z_e a_{e1} + Z_{cf} \alpha_{cf1}}{Z_e \alpha_{e2} + Z_{cf} \alpha_{cf2} + \dfrac{k_2 k_3^*}{2A_S (k_2 + k_3^*)}} \tag{16.b}$$

In these formulae :

$$Z_e = \ell_e^3 / w_e t_e^3 \qquad Z_{cf} = \ell_{cf}^3 / w_{cf} t_{cf}^3$$

$$\alpha_{e1} = 1{,}5\alpha_e - 2\alpha_e^3 \qquad \alpha_{cf1} = 1{,}5\alpha_{cf} - 2\alpha_{cf}^3$$

$$\alpha_{e2} = 6\alpha_e^2 - 8\alpha_e^3 \qquad \alpha_{cf2} = 6\alpha_{cf}^2 - 8\alpha_{cf}^3$$

$$\ell_e = 2(m_e + 0{,}75 n_e) \qquad \ell_{cf} = 2(m_e + 0{,}75 n_1)$$

$$2w_e = b_e \qquad 2w_{cf} = e_2 + 1{,}5 n_e$$

$$\alpha_e = 0{,}75 n_e / \ell_e \qquad \alpha_{cf} = 0{,}75 n_1 / \ell_{cf}$$

All the geometrical properties are defined in Figure 14.

These expressions apply in a similar way to flange cleated connections.

Their validity has been demonstrated in [1] on the basis of a quite large number of comparisons with test results on joints with end-plate and flange cleated connections got from the international literature.

4.2 Simplified stiffness coefficients for inclusion in Eurocode 3

The application of the T-stub concept to a simplified stiffness calculation - as that to be included in a code such Eurocode 3 - requires to express the equivalence between the actual component and the equivalent T-stub in the elastic range of behaviour and that, in

a different way then at collapse; this is achieved through the definition of a new effective length called $\ell_{eff,ini}$ which differs from the ℓ_{eff} value to which it has been referred to in Section 3. In view of the determination of stiffness coefficients k_i, two problems have to be investigated :

- the response of a T-stub in the elastic range of behaviour;
- the determination of $\ell_{eff,ini}$.

These two points are successively addressed thereunder.

4.2.1 T-stub response

The T-stub response in the elastic range of behaviour is covered in section 4.1. The corresponding expressions are rather long to apply; we have therefore introduced some simplifications :

- to simplify the formulae : n is considered as equal to 1,25 m (m and n are indicated in Figure 18.a);
- to dissociate the bolt deformability (Figure 18.c) from that of the T-sub (Figure 18.b).

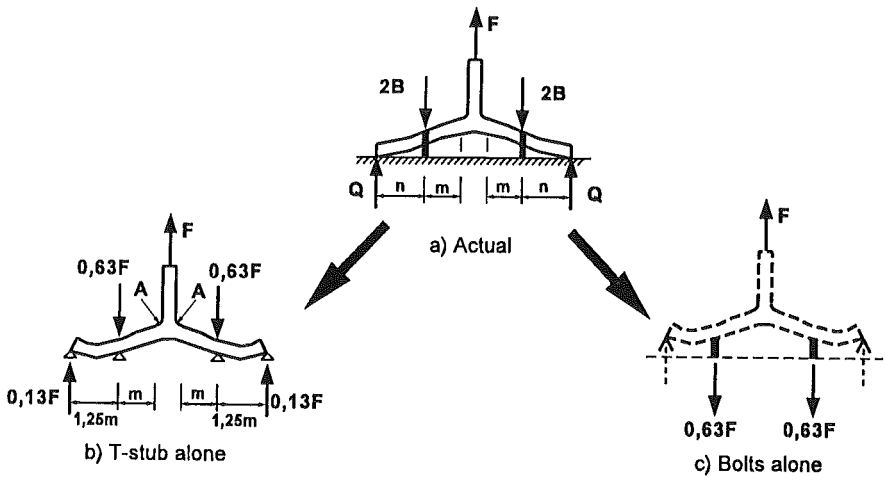

Figure 18 Elastic deformation of the T-stub

Let us first consider the T-stub representing the end-plate. The value of q given by expressions (16) may be simplified to :

$$q = \frac{\alpha_{e1}}{\alpha_{e2}} = \frac{1{,}5\alpha_e - 2\alpha_c^3}{6\alpha_e^2 - 8\alpha_c^3} \tag{17}$$

as soon as it is assumed, as in Figure 18.b, that the bolts are no more deforming in tension $(A_s = \infty)$ and the T-stub is attached to a rigid foundation $(Z_{cf} = 0)$. q further simplifies to :

$$q = 1{,}282 \tag{18}$$

by substituting *1,25* m_c to *0,75* n_c as assumed previously.

The stiffness coefficient given by formula (15.b) therefore becomes :

$$k_{i,e} = \frac{193{,}64}{Z_e} = \frac{193{,}64 t_e^3 \ell_{eff,ini,e}}{2(4{,}5m_e)^3}$$

The effective length $\ell_{eff,ini,e}$ has been substituted to *2* w_e.

Finally :

$$k_{i,e} = 1{,}063 \frac{\ell_{eff,ini,e} t_e^3}{m_e^3} \approx \frac{\ell_{eff,ini,e} t_e^3}{m_e^3} \tag{19}$$

A similar expression may be derived for column flanges or flange cleats in bending, and more generally to any plated component :

$$k_{i,pc} = \frac{\ell_{eff,ini} t^3}{m^3} \tag{20}$$

In the frame of the assumptions made, it may be shown that the prying effect increases the bolt force from 0,5 F to 0,63 F (Figure 18.c). In Eurocode 3, the deformation of a bolt in tension is taken as equal to :

$$\Delta_b = \frac{BL_b}{EA_s} \tag{21}$$

where : $L_b = \Sigma t + \ell_w + \frac{\ell_n}{2} + \frac{\ell_h}{2}$ (see Figure 18)

Σt is the total thickness of the connected plates.

By substituting B by *0,63* F in (21), the stiffness coefficient of a bolt row with two bolts may be derived :

$$k_{i,b} = 1{,}6 \frac{A_s}{L_b} \tag{22}$$

This expression characterizes the deformation of a bolt in tension and applies to non-preloaded bolts where the whole tensile force applied locally by the plate is transferred to the bolts.

In connections with preloaded bolts, the tension force in the bolts increases in a reduced proportion of the force applied by the plate because of the compensation effect of the reduction of the contact forces between the connected plates.

In Figure 18, the force applied in the bolt area equals *0,63 F*; it may be easily shown that a proportion of $\frac{1}{\xi+1}$ will be transferred by the bolt to the foundation, where ξ is the ratio between the axial stiffness of the effective part of the plate subject to contact forces and the stress area of the bolt shank. According to Agerskov [6], the value of ξ may be taken as equal to 5.

As a conclusion, the bolt elongation is seen to be quite lower in connection with preloaded bolts and higher stiffness coefficient can therefore be associated to bolts in tension :

$$\Delta_b = \frac{0{,}63FL_b}{(\xi+1)EA_s} \tag{23}$$

$$k_{i,b} = 1{,}6(\xi+1)\frac{A_s}{L_b} \approx 9{,}5\frac{A_s}{L_b} \tag{24}$$

For consistency with the resistance calculation, only the expression (22) has been included in the revised Annex J of Eurocode 3. It is therefore recommended there for connections with and without preloaded bolts.

4.2.2 Definition of $\ell_{eff,ini}$

In Figure 18.b, the maximum bending moment in the T-stub flange (points A) is expressed as M_{max} = *0,322 F m*. Based on this expression, the maximum elastic load $F_{e\ell}$ (first plastic hinges in the T-stub at points A) to be applied to the T-stub may be derived :

$$F_{e\ell} = \frac{4\ell_{eff,ini}}{1{,}288m}\frac{t^2 f_y}{4\gamma_{M0}} = \frac{\ell_{eff,ini}t^2}{1{,}288m}\frac{f_y}{\gamma_{M0}} \tag{25}$$

In Annex J, the ratio between the design resistance and the maximum elastic resistance of each of the components is taken as equal to 3/2 so :

$$F_{Rd} = \frac{3}{2}F_{e\ell} = \frac{\ell_{eff,ini}t^2}{0{,}859m}\frac{f_y}{\gamma_{MO}} \tag{26}$$

As, in Figure 18.b, the T-stub flange is supported at the bolt level, the only possible failure mode of the T-stub is the development of a plastic mechanism in the flange. The associated failure load is given by Annex J as :

$$F_{Rd} = F_{Rd,1} = \frac{\ell_{eff,1} t^2 f_y}{m \gamma_{Mo}} \tag{27}$$

where ℓ_{eff} is the effective length of the T-stub for strength calculation.

By identification of expressions (26) and (27), $\ell_{eff,ini}$ may be derived :

$$\ell_{eff,ini} = 0{,}859 \ell_{eff} = 0{,}85 \ell_{eff} \tag{28}$$

Finally, by introducing equation (29) in the expression (20) giving the value of $k_{i,pc}$ for any plated component :

$$k_{i,pc} = \frac{0{,}85 \ell_{eff,1} t^3}{m^3} \tag{29}$$

5. DEFORMATION CAPACITY OF PLATED COMPONENTS

5.1 Basis

As explained in Appendix 2, the deformation capacity of a plated component is largely dependent on its design failure mode :

Mode 1 : quite infinite deformation capacity because of the yielding of the plate in bending;

Mode 3 : quite limited deformation capacity because of the brittle fracture of the bolts in tension;

Mode 2 : intermediate situation where the deformation capacity varies from quite limited values (failure load close to that associated to Mode 3) to rather infinite ones (failure load close to that corresponding to Mode 1).

The need for deformation capacity has been expressed in Chapter 3 - Section on assembly - of the present thesis. Two situations have to be contemplated :

- To reach the design moment resistance of a joint, some internal plastic redistribution of forces may have to take place and this requires a sufficient deformation capacity from the components which experience plasticity.

- To enable yield mechanisms to develop in a structural frame, plastic hinges have to form and rotate; the rotation capacity of hinges forming in the joints result from the

deformation capacity of the joint components which have reached plasticity. The demand is obviously higher in this situation than in the previous one.

To check the suitability of a specific component in both situations would require the evaluation of the required and available deformation capacities and the comparison of these two values. The knowledge in this field is not sufficient to allow such a detailed approach. The practical way to proceed till now is to derive so-called deemed-to-satisfy criteria which ensure - sometimes with over-conservatism - that the available deformation capacity is higher than the maximum deformation which could be required in a specific particular joint.

Such criteria, mainly based on test evidence, have been expressed by Zoetemeijer in [Z3] for plated components in bending :

- A plated component possesses sufficient deformation capacity to allow for plastic redistribution within the joint as long as it fails through Mode 1 or 2.
- A plated component possesses sufficient deformation capacity to allow for plastic redistribution within the frame as long as it fails through Mode 1 only.

The second criterion is obviously more restrictive than the first one.

From these requirements, simple deemed-to-satisfy criteria suitable for inclusion in Eurocode 3 have been derived as shown hereunder. The appropriate use of these criteria is described in Chapter 3 of the thesis and more especially in Section 3.2.3. devoted to the evaluation of the design resistance of structural joints.

5.2 Simple deemed-to-satisfy criteria for Eurocode 3

5.2.1 Criterion for plastic redistribution within the frame

In Figure 7, it is shown that the boundary between Mode 1 and Mode 2 failure modes depends on the type of yield line pattern which is considered : circular or non-circular.

Two criteria should so be derived and the appropriate one should be selected, case by case, according to the yield line pattern which governs the failure.

Such a procedure is not desired from a practical point of view and it has been so decided to extract one single criterion which would be valid for all cases.

A safe attitude would consist in selecting (see Figure 7.b) :

$$\beta \leq \frac{2\gamma}{1+2\gamma} \tag{30}$$

as the boundary. But, in order to avoid over-conservatism, the criteria :

$$\beta \leq 1 \tag{31}$$

has finally been agreed.

As a matter of fact, a close examination of old and more recent experimental results on isolated T-stubs indicates that a quite large deformation capacity may be expected from T-stubs, the Mode 2 failure load of which is close to the Mode 1 one.

From condition (31), a simple criteria may be derived if it is assumed that :

- $n = 1{,}25\,m$ (as in Section 4.2.1)
- $B_{t.Rd} = \dfrac{0{,}9 A_s f_{ub}}{\gamma_{Mb}} = \dfrac{0{,}9 \times 0{,}72 \times \pi \times d^2 \times f_{ub}}{4\gamma_{Mb}}$
  $= \dfrac{0{,}51 d^2 f_{ub}}{\gamma_{Mb}}$
- $\ell_{eff} = 2\pi m$ (circular pattern)

d is the bolt diameter in the unthreaded part of the shank.

As a result, the following deemed-to-satisfy criterion is obtained :

$$t \le 0{,}4d\sqrt{(f_{ub}/\gamma_{Mb})/(f_y/\gamma_{MO})} \qquad (32)$$

where t designates the thickness of the plated component.

By adopting values of γ_{M0} and γ_{Mb} respectively equal to 1,0 and 1,25, the following criterion is finally derived :

$$t < 0{,}36d\sqrt{f_{ub}/f_y} \qquad (33)$$

The values considered for γ_{M0} (=1,0) and γ_{Mb} (=1,25) are those used by Zoetemeijer when he suggested the above-mentioned criteria for deformation capacity. Condition (32) could therefore been re-evaluated now on the basis of presently recommended values of γ_M factors (respectively 1,1 and 1,25). This would lead to a bit less restrictive requirement on the component thickness ($t < 0{,}375d\sqrt{f_{ub}/f_y}$). However, to limit the number of situations where the condition (31) is fulfilled and where, simultaneously, Mode 2 failure is governing, the requirement, as expressed by expression (33), has been included in Eurocode 3 Annex J.

5.2.2 Criterion for plastic redistribution within the joint

The criterion $\beta \le 2$, suggested by Zoetemeijer in [Z3], is based on test evidence and has been derived with the assumption of γ_M values respectively equal to 1,0 and 1,25. By referring to actual γ_M values recommended in the code, the criterion becomes :

$$\beta \le 2.\frac{1{,}0}{1{,}1} \qquad (32.a)$$

$$\leq 1{,}82 \qquad (32.b)$$

For Zoetemeijer, who was not differentiating circular yield line patterns from non-circular ones, to limit β to 1,82 meant that T-stubs reaching failure through Mode 3 ($F_{Rd} = \Sigma B_{t.Rd}$) and Mode 2 (but only those where $F_{Rd} > 0{,}96\Sigma B_{t.Rd}$) had a too limited deformation capacity to allow any redistribution of internal forces within the joint. The coefficient "0,96" is derived from Figure 7.b by assuming again that $n = 1{,}25\ m$.

The situation has changed now as a difference is made between circular and non-circular patterns. To accept condition (32) as a boundary for sufficient deformation capacity would mean that T-stubs with circular yield line patterns and exhibiting a Mode 3 failure would be considered as rather ductile. This is obviously not acceptable at all.

This explains why, in Eurocode 3 Annex J, it has been decided to express the Zoetemeijer's criteria not in terms of a β-limitation, but in terms of a F_{Rd} -limitation. A bolt-row with two bolts is therefore considered as sufficiently ductile to allow a further redistribution on internal forces in the joint (see Section 3.2.3.2. of the present thesis), as long as its design resistance is such that :

$$F_{Rd} \leq 2.0{,}96 B_{t.Rd} \qquad (33.a)$$

$$\leq 1{,}92 B_{t.Rd} \qquad (33.b)$$

In Eurocode 3 Annex J, the criteria has been approximated to :

$$F_{Rd} \leq 1{,}9 B_{t.Rd} \qquad (34)$$

6. CONCLUSIONS

In this Appendix, the user's friendly character of the T-stub approach for plated components has been demonstrated. One of its main features is the possibility to apply a same concept and similar formulae for the strength evaluation and stiffness evaluation of any plated component such as an end-plate in bending, flange cleats in bending or column flanges in bending. Its interest in deriving criteria for sufficient deformation capacity of plated components has also been shown.

The background for possible improvements of the concepts, and in particular the consideration of the beneficial influence of the bolt preloading and of the bolt size on the stiffness and resistance properties of the plated components has been highlighted and validated. Simplified stiffness and resistance formulae taking these effects into account have been proposed. Those covering the influence of the bolt size have been included in the revised Annex J of Eurocode 3 and the format of the expressions showing the effect of bolt preloading is such that a future implementation of these rules in Eurocode 3 Annex J may be contemplated.

7. REFERENCES

[1] Jaspart, J.P.

Etude de la semi-rigidité des noeuds poutre-colonne et son influence sur la résistance et la stabilité des ossatures en acier.

Ph.D. Thesis, Department MSM, University of Liège, 1991.

[2] Yee, Y.L. and Melchers,R.E.

Moment rotation curves for bolted connections.

Journal of the Structural Division, ASCE, Vol. 112, ST3, pp. 615-635, March 1986.

[3] Zoetemeijer, P.

A design method for the tension side of statically loaded bolted beam-to-column connections.

Heron, Delft University, Vol. 20, n° 1, 1974.

[4] Zoetemeijer, P.

Summary of the researches on bolted beam-to-column connections.

Report 6-85-7, University of Technology, Delft, The Netherlands, 1985.

[5] Kishi, N., Chen, W.F., Matsuoka, K.G. and Momachi, S.G.

Moment-rotation relationship of top- and seat-angle with double angle connections.

Connections in Steel Structures, Elsevier Applied Science Publishers, 1988, pp. 121-134.

[6] Agerskov, H.

High-strength bolted connections subject to prying.

Jl. of Struct. Div., ASCE, Vol. 102, ST1, 1976, pp. 161-175.

[7] Zanon, P. and Zandonini, R.

Experimental analysis of end-plate connections.

Connections in Steel Structures. Elsevier Appl. Sc. Publ., 1988, pp. 41-51.

[8] Damiani, A.

Comportamento di giunti semi-rigid in acciaio :analisi sperimentale e methodi di predizione.

Ph.D. thesis, Univ. of Pavia, 1986.

[9] Bursi, O.

Tests and modelling of bolted double clip angles of steel building connections.

Report Univ. of Trento, 1990.

[10] Davison, J.B., Kirby, P.A. and Nethercot, D.A.

Rotational stiffness characteristics of steel beam-to-column connections.

Journal of Constructional Steel Research, Vol. 8, 1987, pp. 17-54.

[11] Hotz, R.

Traglastversuche für Stütze-Riegel-Verbindungen mi verbesserter Wirtschaftlichkeit.

Der Stahlbau, 11, 1983, pp. 329-334.

[12] Douty, R.T., Mc Guire, W.

High strength bolted moment connections.

Journal of the Structural Division, ASCE, vol. 91, n° ST2, avril 1965, pp. 101-128.

[13] Eurocode 3, ENV-1993-1-1, Revised Annex J, Design of Steel Structures, CEN,

Document CEN/TC250/SC3 - N419E, Brussels, June 1994.

[14] Packer, J.A., Morris, L.J.

A limit state design method for the tension region of bolted beam-to-column connections.

The Structural Engineer, vol. 5, n° 10, octobre 1977, pp. 446-458.

[15] Whittaker, D., Walpole, W.R.

Bolted end-plate connections for seismically designed steel frames.

Research report 82-11, Department of Engineering, University of Canterbury, New-Zealand, September 1982.

[16] Zanon, P.

Bolted connections : the ultimate limit state behaviour of end-plates.

Costruzioni metalliche, n° 1, 1985, pp. 40-48.

[17] Surtees, J.O., Mann, A.P.

End-plate connections in plastically designed structures.

Proceedings of the Conference of Joints in Structures, vol. 1, Paper 5, University of Sheffield , England, July 1970, pp. A5.1-A5.18

[18] Kato, B., Mc Guire, W.

Analysis of the T-stub flange-to-column connections.

Journal of the Structural Division, ASCE, vol. 99, n° ST5, mai 1973, pp. 865-888.

[19] Agerskov, H

Analysis of bolted connections subject to prying.

Journal of the Structural Division, ASCE, vol. 103, n° ST11, novembre 1977, pp. 2145-2163.